

30 GHz Broadband Bow-tie Printed Ridge Gap Waveguide Antennas

Syed Muhammad Sifat

A Thesis
In the Department
Of
Electrical and Computer Engineering

Presented in Partial Fulfillment of the Requirements
For the Degree of
Master in Applied Science (Electrical and Computer Engineering) at
Concordia University
Montreal, Quebec, Canada

April 2019

© Syed Muhammad Sifat 2019

CONCORDIA UNIVERSITY
SCHOOL OF GRADUATE STUDIES

This is to certify that the thesis prepared

By: Syed Muhammad Sifat

Entitled: 30 GHz Broadband Bow-tie Printed Ridge Gap Waveguide Antennas

and submitted in partial fulfillment of the requirements for the degree of

Master of Applied Science

Complies with the regulations of this University and meets the accepted standards with respect to originality and quality.

Signed by the final examining committee:

_____	Chair
Dr. Christopher W. Trueman	
_____	Examiner, External
Dr. Farjad Shadmehri (MIE)	To the Program
_____	Examiner
Dr. Christopher W. Trueman	
_____	Supervisor
Dr. Abdel Sebak	
_____	Co-Supervisor
Dr. Shokry Shamseldin	

Approved by: _____

Dr. W. E. Lynch, Chair

Department of Electrical and Computer Engineering

_____ 20 _____

Dr. Amir Asif, Dean

Gina Cody School of Engineering and
Computer Science

Abstract

30 GHz Broadband Bow-tie Printed Ridge Gap Waveguide Antennas

Syed Muhammad Sifat

Concordia University

The development of wireless and satellite communication systems has led to high demand for microwave and millimeter wave application components, which play an essential role in the upcoming 5G communication. The coverage area of such systems is control by transmitted power as well as the antenna gain of the system. Hence, it is essential to design a high gain antenna that can mitigate the losses and extend the system coverage area. Higher frequencies lead to smaller sizes of RF components including antennas. However, the implementation of passive components and guiding structure becomes difficult based on traditional guiding structures such as microstrip lines, and waveguides at millimeter wave bands. Microstrip line suffers from cavity modes, which leads to surface waves and has more losses at higher frequencies. The rectangular waveguide has high power handling capability, low losses, and high Q-factors which makes it very attractive for high-frequency applications. On the other hand, at high frequencies, the wavelengths become challenging to construct with current machining techniques as ensuring good electrical contact become very challenging.

In this thesis, planar high gain antennas are designed based on Printed Ridge Gap Waveguide (PRGW). The primary objective of this work is to develop high gain, wideband antennas that can support the future demand for high data transmission. Therefore, a detailed analysis for PRGW has been introduced as well as featured designs of the high

gain antenna. This antenna array can perform for future 5G communication purpose, and it fulfills all the requirements of mm-wave bands.

In this work, a groove-based wideband bow-tie slot antenna array is designed at 30 GHz based on printed ridge gap waveguide technology (PRGW). A two-section T-shaped ridge is designed to feed a bow tie slot placed on the upper ground of PRGW. The gain of the proposed slot antenna is enhanced by using a horn-like groove. Then, the proposed high gain element is deployed to build up a 1 x 4 bow-tie slot antenna array loaded with three-layer groove antenna. The proposed antenna array is fabricated and measured, where the measured results show a -10 dB impedance bandwidth from 29.5 to 37 GHz (22%). The fabricated prototype achieves a high gain of 15.5 dBi and a radiation efficiency higher than 80% over the operating frequency bandwidth. Besides, to reduce the edge diffraction in the E-plane, an artificial corrugation ring is deployed with a certain depth so that it can improve the overall antenna performance.

Dedication

I want to dedicate this work to the 3 million martyrs who sacrificed their lives during the 1971 Liberation War in Bangladesh and to all those people who are fighting for their freedom, liberty and human rights in Palestine, Syria, Myanmar, Somalia, and Baluchistan.

Acknowledgements

I want to express my sincere thanks to my supervisor, Prof. Abdel-Razik Sebak for all his guidance and support throughout the whole master's program.

I am thankful to Prof. Ahmed Kishk, and Prof. Robert Paknys for their outstanding lectures during my courses which developed me to understand the fundamentals very well and I would like to thank the committee members for reviewing my thesis.

My heartiest thanks to my Co-supervisor Dr. Shoukry Shamseldin for sharing his knowledge and for his continuous motivation, support, and feedback about my work which helped to complete my thesis within time. I want to thank my colleagues from our research group especially Nadeem Ashraf, Mamdooh Ali, Islam Afifi and finally my friends Dhruva Kumar, Yazan Al-Alem and Reza Rahimi (Polytechnic Montreal). I also like to thank Vincent Chopin & Jeff Landry for their technical assistance in the fabrication.

At last, I would like to thank my parents for their love, my beloved wife, Fariyan for her support & encouragement and Almighty Allah without whom this wouldn't have been possible.

Table of Contents

List of Figures	x
List of Tables	xiii
List of Abbreviations	xiv
Chapter 1: Introduction	1
1.1 Development of Wireless Communication	1
1.2 Evolution of mobile communication	2
1.3 Millimeter-wave Characterisations	3
1.4 Guiding Structures in mm-wave band	5
1.5 Motivation of the Thesis	6
1.6 Objective of the Thesis	7
1.7 Thesis Organization	8
Chapter 2: Literature Review	9
2.1 Introduction	9
2.2 Millimeter-Wave Antennas	9
2.2.1 Microstrip Antennas	9
2.2.2 Horn Antenna	11
2.2.3 Substrate Integrated Waveguide Based Antennas	12
2.3 Theoretical Background of Gap Waveguide Technology	13
2.3.1 Soft and Hard Surfaces	13
2.3.2 Artificial Magnetic Conductors (AMC) textured surfaces	14
2.3.3 Operation Principle and Architectures of Gap Waveguides	15
2.3.4 Ridge Gap Waveguide	16
2.3.5 Unit cell analysis	17
2.4 Some other type of Gap Waveguide	18
2.4.1 Groove Gap Waveguide	18

2.4.2	Inverted Microstrip Gap Waveguide	19
2.5	Ridge Gap waveguide Based Antennas	20
2.6	Bow-tie Antenna	22
2.7	Summary	23

Chapter 3: Proposed Single Element Bow-tie Gap Slot Antenna with PRGW **25**

3.1	Design Methodology	25
3.2	Printed Ridge Gap Waveguide	26
3.3	RGW Excitation	28
3.4	Operating modes of RGW	30
3.5	Field Distribution along RGW	31
3.6	Applications of RGW	32
3.7	Printed Ridge Gap Waveguide Antenna	33
3.7.1	PRGW Antenna using linear slot	33
3.7.2	T-shaped Ridge along with multi-section transformers	34
3.8	Bow-tie Antenna with two section T-shaped Ridge	35
3.9	Three-layer Horn-like Groove Antenna with Bow-tie Slot	37
3.10.1	Bow-tie shaped Ridge Slot Antenna augmented with Superstrate	41

Chapter 4: Proposed Bow-tie Slot Antenna Array Based on PRGW **45**

4.1	Antenna Arrays for High gain Applications	45
4.2	Power Divider based on PRGW	46
4.2.1	1 x 4 Power divider based on PRGW	46
4.2.2	E-field Distribution of 1 x 4 Power divider based on PRGW	47
4.3	1 x 4 Bow-tie Slot Antenna Array based on PRGW	48
4.4	1 x 4 Groove Antenna Array with Corrugation Ring	51
4.5	Experimental and Validation	55

Chapter 5: Conclusion and Future Works	60
5.1 Conclusion	60
5.2 Future Works	61
References	62

List of Figures

1.1	Atmospheric attenuation at different frequency bands	4
2.1	Typical feeds of Microstrip patch antennas (a) Co-axial probe feed	
	(b) Microstrip Line feed. (c) Aperture coupled feeding technique.	10
2.2	3-D Structure of Pyramidal horn antenna with and without corrugations ...	11
2.3	Designed Structure of Substrate Integrated Waveguide	12
2.4	(a) Bed of nails in the bottom plate	
	(b) Mushroom type EBG patches in a dielectric substrate	15
2.5	(a) PEC-PMC parallel plate	
	(b) Ridge surrounded by PEC/PMC plates	16
2.6	Ridge surrounded by bed of nails.	17
2.7	Unit cell of a ridge gap waveguide structure	18
2.8	(a) Cross section of Groove gap waveguide.	
	(b) 3-D Structure of Groove gap waveguide	19
2.9	(a) Cross section of Inverted Micro-strip Gap waveguide	
	(b) Complete structure of inverted micro-strip gap waveguide	20
2.10	Metal Ridge Gap Waveguide Antenna	22
3.1	Flowchart of Proposed Work	25
3.2	Proposed structure of the printed ridge gap waveguide.	27
3.3	One row of unit cell with ridge.	27
3.4	Dispersion diagram with the ridge existence	28
3.5	(a) Microstrip to Ridge transition.	
	(b) Simulated S-parameter of the PRGW Transition	29
3.6	Electric & Magnetic field distribution from the port end	30
3.7	Field distribution of PRGW using Microstrip transition at various frequencies	31
3.8	PRGW Antenna with linear slot	33
3.9	Reflection Coefficient of the simulated slot antenna using PRGW	34
3.10	PRGW slot antenna with a T-shaped ridge	35

3.11	Reflection Coefficient of two section T-shaped ridge with PRGW	35
3.12	3-D structure of two section T-shaped ridge based on PRGW	36
3.13	(a) Proposed 3D model for the single element bow-tie groove		
	(b) Feeding layer		
	(c) Bow-tie slot antenna layer		
	(d) Horn-like groove layer	37
3.14	(a) Simulated reflection coefficient of single element PRGW antenna		
	(b) Gain versus the frequency comparison for the single element antenna		39
3.15	Simulated radiation pattern comparison for single element antenna at 30 GHz.	40
3.16	Simulated gain comparison by changing groove size	41
3.17	Proposed design of bow-tie shaped ridge along with parameters	...	42
3.18	Proposed bow-tie antenna with superstrate	43
3.19	(a) Simulated reflection coefficient of bow-tie slot antenna		
	(b) Gain versus frequency response with and without the superstrate	...	43
4.1	(a) Layout of 1 x 4 power divider		
	(b) S-parameter of the power divider	47
4.2	E- field distribution of 1 x 4 power divider using PRGW at 30 GHz	48
4.3	(a) Simulated model top view of the bow-tie slot antenna array		
	(b) Simulated reflection coefficient and gain of 1× 4 bow-tie antenna array		49
4.4	Simulated normalized radiation pattern for 1 x 4 bow-tie antenna array		
	(a) E-plane (b) H-plane	50
4.5	(a) Proposed 1 x 4 three layer groove array antenna	51

	(b) Simulated reflection coefficient and gain of 1 x 4 groove antenna array	51
4.6	Simulated normalized radiation pattern for 1 x 4 linear array (a) E-plane	
	(b) H-plane	52
4.7	Improved 3-D, 1 x 4 groove antenna array with a corrugation ring	53
4.8	Simulated normalized E-plane radiation pattern using a corrugation ring	
	(a) 32 GHz. (b) 34 GHz.	54
4.9	(a) Prototype Layers	
	(b) Final assembly of 1 x 4 integrated antenna array	55
4.10	(a) Measured reflection coefficient of the fabricated 1 x 4 antenna array	
	(b) Radiation pattern measurement setup in the anechoic chamber ...	56
4.11	Measured gain of the fabricated 1 x 4 antenna array	57
4.12	Comparison of measured and simulated E and H-plane radiation pattern	
	(a) E-plane at 30 GHz	
	(b) H-plane at 30 GHz	57
4.13	Comparison of measured and simulated E and H-plane radiation pattern	
	(a) E-plane at 34 GHz	
	(b) H-plane at 34 GHz	58

List of Tables

2.1	Comparison of different antenna configurations with different technologies.	24
3.1	Designed parameters for the proposed PRGW Antenna	38
3.2	Dimensions of PRGW Bow-tie shaped ridge with slot (in mm)	42
4.1	Dimensions of PRGW antenna array (in mm)	49
4.2	Comparison of proposed antenna with some previously published work.	59

List of Acronyms

1D	One-Dimensional
3D	Three-Dimensional
5G	Fifth Generation
AMC	Artificial Magnetic Conductor
BW	Bandwidth
CST MWS	Computer Simulation Technology Microwave Studio
DRA	Dielectric Resonator Antenna
DUT	Device under Test
EBG	Electromagnetic Band Gap
EM	Electromagnetic
FEM	Finite Element Method
FDTD	Finite Difference Time Domain
FSS	Frequency Selective Structure
HFSS	High Frequency Structure Simulator
IOT	Internet of Things
MSL	Microstrip Line
MMW	Millimeter- Wave
MIMO	Multiple Input Multiple Output
PEC	Perfect Electric Conductor
PCB	Printed Circuit Board
PMC	Perfect Magnetic Conductor
RGW	Ridge Gap Waveguide
SIW	Substrate Integrated Waveguide
SLL	Side Lobe Level
TE	Transverse Electric Wave
TEM	Transverse Electromagnetic Wave
TM	Transverse Magnetic Wave
TSA	Tapered Slot Antenna

Chapter 1

Introduction

1.1 Development of Wireless Communications

In the last decade, the communication world has experienced a real revolution which was just a dream before. The technological advancement in the communication sector has led us to this stage through the secure wireless network, signal integrity in communications and high-performance antennas. In the 1970s, the Bell lab devised a cellular system and developed first standards to be commercially applicable and usable. The growth of demand increased more in commercial applications during the 1980s and 90s that helped to deploy modern wireless mobile services. During this journey, technological advancement increased significantly with the high consumer demand, while mobile communications are expected to reach 5G within 2020 [1]. With the help of the current wireless networks, it is possible to connect to the internet from mobile phones, tablets, and laptops. Nowadays it is feasible to watch football, hockey on live streaming because of high-speed internet connectivity. Information and communication technology has advanced enough to have significant impacts on all aspects of life.

Wireless data transfer is not only limited to communication purposes, but also it has a significant impact on medical, surveillance, and radio broadcasting. For higher data transmission, the wide bandwidth is mandatory which can be realized by the utilization of upper-frequency bands. This fact directs both the industry and the research community to the millimeter-wave bands [2].

1.2 Evolution of Mobile Communication

In the last four decades, the telecommunications industry has seen significant advances in technology. Mobile communication evolved first in the 1980s, where 1G was launched only for voice communication purpose. Afterward, the second generation (2G) communication was introduced in the early 90s, which had a speed of 64 kbps based on digital signals for voice transmission supporting short message services (SMS), conference calls, and call holding. Hence, the third generation, 3G communication was introduced at the early 2000s for both voice and video transmission. For high data transmission and radio broadcasting 4G was launched offering a download speed of 100 Mbps. Although the mobile communication systems have gone through this revolution, the dynamic needs of the customer encourage for more developments [2, 3].

5G communication is expected to provide a clear difference and add more services over 4G. Although the LTE (4G) systems show superior performance, the human needs are still asking for more enhancements. Communication systems research and development are directed to enable the future application with a massive number of users such as IoT and ultra-wideband applications such as virtual reality which motivates the research towards a new mobile generation. This generation is expected to be released around 2020 enabling, uninterrupted access to information, entertainment, and communication [3, 4].

Normally mobile communication operates at frequencies between 800 MHz to 3 GHz. At this frequency bands, the propagation and attenuation losses are low, as a result, long-distance coverage can be assured. On the other hand, it has a limited bandwidth to support the need for a large number of users [5]. Hence, one of the most recommended solutions is

the operation at the millimeter wave band (30-300 GHz), despite, the high attenuation and propagation losses compared to lower frequency bands. To mitigate this loss high gain antennas are needed so that it can compensate for the expected losses [6]. In the next section, we will discuss mm-wave applications in more detail.

1.3 Millimeter-wave Characterisations

The millimeter wave range includes frequency from 30 to 300 GHz, with wavelengths between 10mm to 1mm. At this frequency band the propagating signal suffers from high absorption losses; as a result, it limits to short distance communication. The mm-wave bands have many advantages such as [7]: Mature communication technology

- Optimum for short distance communication.
- High level of frequency re-use.
- Small sized antenna.
- Unlicensed operation with low interference.

Millimeter-Wave is subjected to more propagation losses compared to lower frequency bands, due to the oxygen absorption level at mm-wave. On the other hand, there are plenty of technical, mechanical and environmental factors like (rain, stormy weather, etc.) which degrades the overall performance of the antenna at mm-wave bands. Some of the critical factors that affect millimeter wave propagation are given below [8].

- Atmospheric Gases Attenuation: Water vapor absorption and Oxygen absorption.
- Rain.
- Diffraction (Bending).
- Scattering effects (Reflections, diffusion).

As the frequencies increase, the wavelength becomes shorter, and the reflective surface appears rougher, which results in more diffused reflection as opposed to specular reflection [8]. The mm-wave band is considered as a potential candidate for the upcoming 5G communication system as it supports a massive amount of unlicensed spectrum. Fig. 1.1 shows atmospheric attenuation at different frequencies [9].

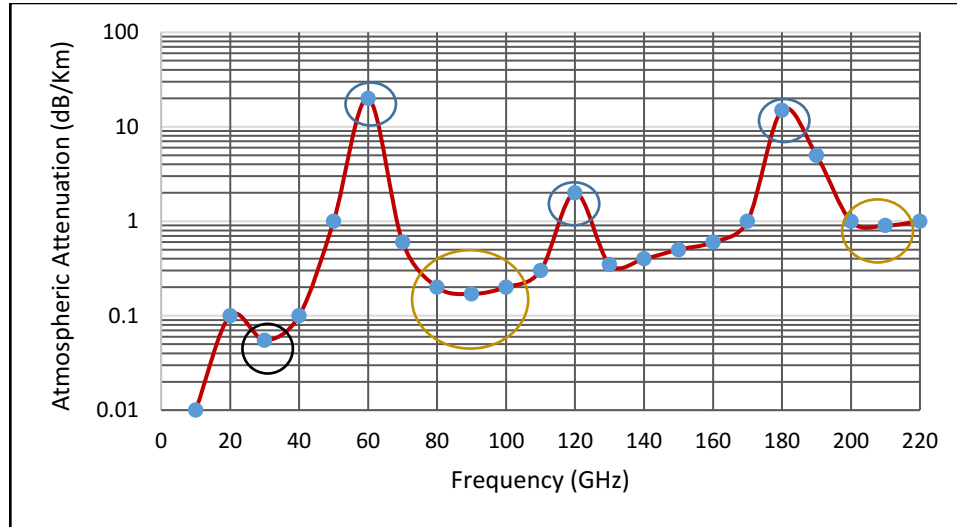


Figure 1.1: Atmospheric attenuation at different frequency bands [9].

As the frequency increases the air attenuation increases as indicated clearly in the shown figure. Especially, for 60 GHz, where the attenuation is very high and makes it suitable for short-range communications. The carrier frequency at 60 GHz delivers unprecedented data rates, several tens of gigabits per second, allowing high definition data transfer, sensing and radar applications [7]. In the following section, various waveguide structures will be discussed, where the performance of these structures will be highlighted especially in the mm-wave band.

1.4 Guiding Structures in mm-wave band

One of the most exciting and challenging parameters in Microwave/RF systems is the hosting guiding structures. In MHz range, transmission lines are used mostly where the signal carries in the form of TEM mode. As the frequency increases the transmission losses increases due to sheet resistance, which is linearly proportional to the square root of the frequency. Air filled waveguides are a low loss guiding structure with high power handling capability. Circular waveguides and rectangular waveguides are the most popular air filled waveguides for high-frequency applications. The rectangular waveguide is the most common guiding structure for high-frequency applications, and the losses are low compared to any other guiding structures because of its high Q-factor. The rectangular waveguide has a hollow tube inside where the wave travels. At mm-wave bands, it is challenging to construct a rectangular waveguide because of its sidewalls. With an increase in frequency the dimensions get smaller; as a result, conventional machining becomes complex and less accurate. Hence, the proper electrical contact between the plates becomes more challenging.

Strip lines, microstrip lines, are suitable for low-frequency applications. As they are print on a dielectric substrate, it suffers from high dielectric losses at high-frequencies [10]. Besides, at higher frequencies in microstrip lines, it suffers from high cavity modes and surface waves which leads to unwanted radiation. The mentioned drawbacks, significantly affect the suitability of microstrip lines in mm-wave bands. The co-planar waveguide is another type of planar waveguide which constructs on a dielectric substrate, which is also preferable for low-frequency application.

In the last decades, lots of work had been done to propose and analyze modern guiding structure suitable for mm-wave applications, such as substrate integrated waveguide (SIW), ridge gap waveguide (RGW) and the packaged microstrip line. The operating mode of SIW is similar to the rectangular waveguide, which makes it a reasonable extension of the rectangular waveguide. SIW is a planar structure where the field travels in the substrate between the two rows of via holes replacing the sidewalls of a rectangular waveguide [11, 12]. This structure has many advantages as it is low profile and can be integrated easily with other system parts on a single board. On the other hand, SIW suffers from dielectric losses and dispersive propagation.

Another promising candidate for mm-wave applications is the Printed Ridge Gap Waveguide (PRGW). PRGW is the printed version of ridge gap waveguide, where the bottom layer is plated using mushrooms and vias which controls the electromagnetic bandgap of the overall structure. PRGW is analyzed, and later on, a high gain antenna is designed based on this concept. In the next section, some basic ideas about the new guiding structure shall be discussed in more details.

1.5 Motivation of the Thesis

The design challenges for wireless communication in mm-wave frequencies is to realize an overall system with low loss, compact size, and cost-effectiveness at the same time. Gap waveguide technology first emerged in 2009 by Kildal [13], where the necessary cut-off of a PEC-PMC parallel plate configuration was used to control the electromagnetic wave propagation between two parallel plates. As long as the air gap separation between the two PEC-PMC plates is less than $\lambda/4$, there won't be any wave propagation, which controls the

electromagnetic bandgap of the structure. If the bottom surface incorporates a ridge, then the wave propagation will be within the ridge only. However, the textured AMC surface must also include guiding structures in the form of ridge, grooves or strips to form a complete waveguide.

Based on the previous discussion RGW is considered among the expected candidates for future applications due to its low losses and low dispersion. The RGW has shown promising results; however, the need for high accuracy CNC machining is a significant drawback for this configuration. As a result, many articles were published to propose a printed version of RGW for better integrability and lower cost.

1.6 Objective of the Thesis

The objectives of this work is divided into three sections.

- The primary objective of this work is to design a high gain antenna with very wide-bandwidth to support high data transmission that is one of the main focus to work at the mm-wave band.
- The second objective contains the gain enhancement technique using the PRGW array antenna and the integration between the feeding network arrays with a grooved layer.
- The last goal of this work is to improve the overall efficiency and radiation pattern using one layer a corrugating ring with a certain depth, which enhances the total performance of the antenna array.

This thesis presents the development of PRGW antennas for mm-wave applications.

1.7 Thesis Organisation

Chapter 2, provides a literature review on various types of antennas which is followed by a detailed discussion of hard and soft surfaces, periodic structures which will introduce the concept of Gap Waveguides, along with some other types of gap waveguides. *Chapter 3*, presents a novel antenna analysis and design based on PRGW along with the bandwidth enhancement through the multi-section transformer. *Chapter 4*, highlights the feeding network using PRGW technology where the proposed array structure exceeds 16 dBi gain. Finally, *chapter 5* summarize the thesis outcomes as well as suggest valuable extensions as future work.

Chapter 2

Literature Review

2.1 Introduction

The history of millimeter wave communication is not that recent. Despite mm-wave technology having established for many decades, the mm-wave systems have only deployed for military applications. With advances in process technologies and low-cost integration solutions, this technology has started to gain a great deal of momentum from academia and industries. In this chapter a brief overview of different types of antennas will be described; afterward, mm-wave antennas will be covered in brief.

2.2 Millimeter Wave Antennas

There is a growing interest in mm-wave antennas because of the demand for high data rate communication applications. In this section, antennas that are well suited for mm-wave applications will be discussed. Some of the notable antennas in mm-wave range are microstrip antennas, horn antennas, substrate integrated waveguide (SIW) based antennas will be discussed.

2.2.1 Microstrip Antennas

The microstrip antenna is among the commonly used antenna for satellite and wireless communications. It is print on the substrate, which makes the structure planar, low profile, cheap, and most importantly it is easy to fabricate. For bandwidth enhancement, a lot of techniques were proposed [14-17]. It is possible to obtain both end-fire and broadside radiation pattern from microstrip antennas. A microstrip patch antenna gives broadside

radiation pattern with a very directive beam width. The coaxial probe, microstrip Line, and aperture coupled method are the three commonly used feeding techniques which are illustrated in Fig. 2.1.

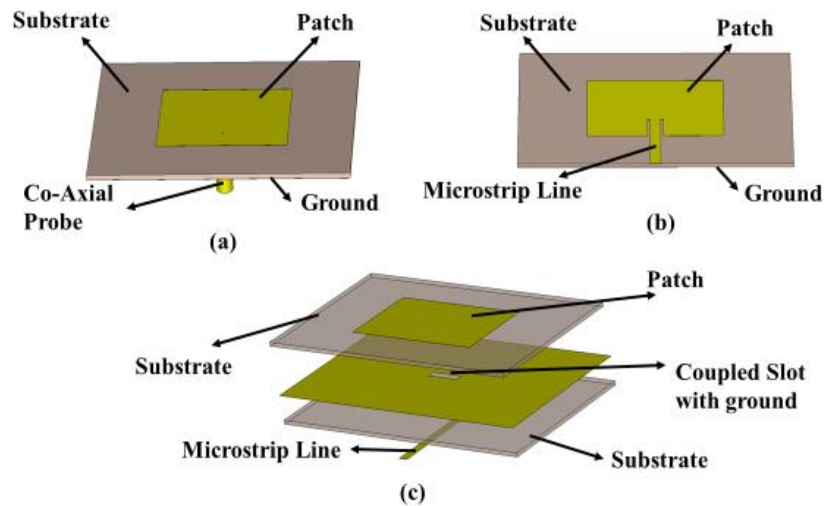


Figure 2.1: Typical feeds of Microstrip patch antennas. (a) Co-axial Probe feed, (b) Microstrip Line feed, (c) Aperture coupled feeding technique.

The thickness of the substrate is kept very thin so that it is possible to reduce surface waves, which leads to significant radiation. In general, a patch antenna gives broadside radiation, and the bandwidth of the antenna is 2-5% at the center frequency. Extensive work has been proposed to improve the bandwidth of the patch antenna, and one of the techniques is stacked patches [16]. Stacked patches were designed to cover the whole Ka-band, where the reflection coefficient is < -10 dB from (27-40) GHz giving broadside radiation of 6 dB covering the entire frequency band [17].

Ultra-wideband (UWB) Antennas are planar, low profile antennas with large bandwidth which almost covers the whole operating frequency range of the system and mostly gives

a very stable radiation pattern. In this section, some UWB antennas which is used for low-frequency applications will discuss at first, and later on, high-frequency application UWB antennas will be covered [18-20]. Printed log periodic dipole array (PLPDA) antenna also falls into the category of UWB antennas and can be used to give broadband & high gain. PLPDA antenna with several parasitic bowtie directors was used to reduce the side lobes and enhance the antenna performance [21]. Besides, PLPDA antenna with corrugations was proposed, for high gain, wideband applications [22].

2.2.2 Horn Antenna

Horn antenna is one of the simplest and probably the most widely used microwave antenna all over the world. It is used in radio astronomy, satellite communication, and communication dishes. It has a very directive radiation pattern. In terms of gain and bandwidth, a horn antenna is the most suitable antenna for mm-wave applications. There are different types of horn antennas like the E-plane sectoral horn, the H-plane sectoral horn, pyramidal horn, and circular horn antenna [23, 24]. The most common one is the pyramidal horn which is flared in both E and H-plane as illustrated in Fig. 2.2

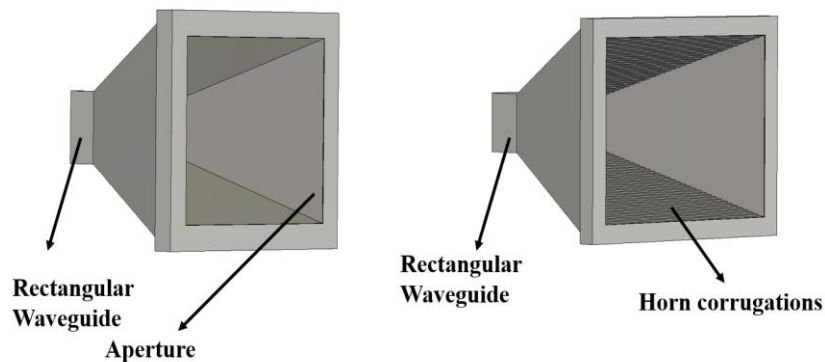


Figure 2.2: 3-D structure of pyramidal horn antenna with and without corrugations.

Corrugated horns are used to reduce to cross polarization and side lobe level. Some articles proposed the idea of a soft and hard surface to obtain a symmetric radiation pattern, which increased the gain of the antenna [25]. Also, the multilayer SIW pyramidal horn antenna was designed to get 12 dB gain with PCB technology for mm-wave application [26]. Integrated horn antenna array consists of dipole antennas suspended on dielectric membrane inside a pyramidal cavity etched in silicon [27]. Metallic horn antenna is bulky and expensive to fabricate, and it is not suitable for all the applications because of its non-planar structure.

2.2.3 Substrate Integrated Waveguide based Antenna

In the last decade, there was an increasing demand for work in Substrate Integrated Waveguide (SIW) technology as a guiding structure. It is a low profile, a planar structure which makes it very suitable for beamforming applications. In SIW instead of the sidewalls metallic, vias are used, which guides the fields traveling in the substrate as illustrated in Fig. 2.3.

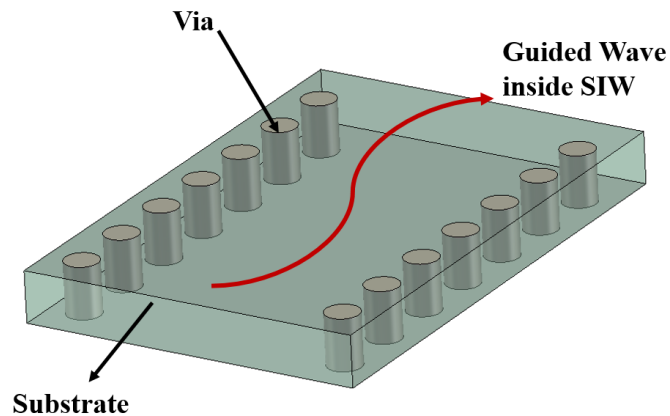


Figure 2.3: Designed Structure of Substrate Integrated Waveguide.

SIW is built on a substrate, and it can be used as an extension of rectangular waveguide [28]. At high frequencies, it is often difficult to construct rectangular waveguide, mainly because of the sidewalls. Besides, SIW based antennas possess low attenuation losses at higher frequencies because of the high Q-factor. A circular polarized X-shaped slot was used to get circular polarization at 36.5 GHz, and a high gain was achieved [29].

To diminish the radiation loss over long distance communication sequential feeding network via-SIW was suggested which minimizes the radiation losses and it shows significant improvement in terms of bandwidth and gain [30]. SIW cavity-backed antennas demonstrated on a single layer substrate where grounded CPW uses as a feeding line to the cavity [31]. Although, the performance of the SIW seems better than some other existing technologies like microstrip lines and coplanar waveguides; however it suffers from high dielectric losses at mm-wave bands. In the next section, we will discuss about “Gap Waveguides” a new technology that is well suited for mm-wave frequency band because of its high Q-factor & low loss and it does not require any sidewalls as a rectangular waveguide.

2.3 Theoretical Background of Gap Waveguide Technology

2.3.1 Soft and Hard surfaces

Soft and hard surface are metamaterials that artificially support magnetic conductivity [32]. Generally, a soft surface stops the wave from propagating, and hard surface supports the wave to propagate. These characteristics are deployed in corrugated horn antennas to reduce the side-lobe level, couplings, and cross polarization, and the depth of the groove

usually are kept $\lambda / 4$ [33]. On the contrary, for hard surfaces, the corrugation with a depth d must be filled with a dielectric material that has a dielectric constant more substantial than the permittivity of the medium above the surface. The depth of the corrugation can be represented using the equation below,

$$d = \lambda / 4 \sqrt{\epsilon_r - 1} \dots\dots\dots (1)$$

Where λ is the free space wavelength, ϵ_r is the dielectric constant of the material. This concept is used in hard waveguide horns to increase aperture efficiency [34]. Ideally, soft and hard surfaces can be recognized using PEC/PMC strips. For a hard surface, the wave will propagate when the strip and direction of propagation are both in the longitudinal direction. On the other hand, a soft surface can stop any wave for any polarization which is transverse to the strip direction. To be more specific, the strip or the corrugation will cancel both transverse electric and magnetic field components. As a result, of elimination of both the transverse field components the field propagation will also be stopped.

2.3.2 Artificial Magnetic Conductors (AMC) textured surfaces

There is no such thing as perfect magnetic conductor (PMC) in reality; however, it is possible to get artificial magnetic conductivity by using periodic structures in both two-dimensional spaces. EBG will stop the wave propagation of all polarizations in all direction parallel to the surface as it has a 2D periodicity. EBG can be realized using in a textured structured made of metal pins which are known as ‘bed of nails’ [35]. The two most common EBG structures are the bed of nails and the mushroom structure which illustrates in Fig. 2.4 where the ground is kept hidden for better understanding.

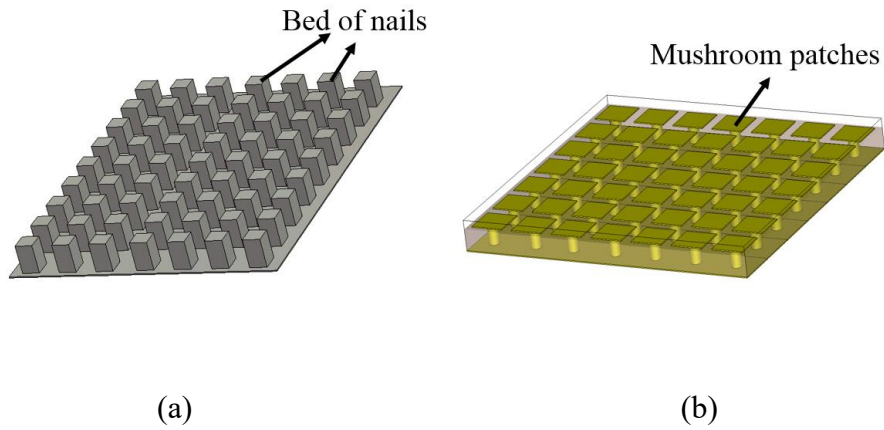


Figure 2.4: (a) Bed of nails in the bottom plate, (b) Mushroom type EBG patches in a dielectric substrate.

To form an AMC surface, the height of the pins will be in a range of $\lambda / 4$ at the center frequency of the operating bandwidth. For Fig. 3.2 (b), the surface may consist of an array of periodic patches of different shapes (square, circular, hexagonal, etc.) is placed above a substrate and is connected to the ground plane by posts through vias or pins. The height of the substrate is usually less than a tenth of a wavelength ($h < \lambda / 10$), where the vias are necessary to suppress surface waves within the substrate. The stopband of a periodic bed of nails is measured with some numerical analysis to form a relationship with the dispersion diagram [36].

2.3.3 Operation Principle and Architectures of Gap Waveguides

Kildal developed the idea of gap waveguide technology in 2009 [13]. The operation principle is similar to a PEC-PMC parallel plate waveguide. Between the PEC/PMC plates, no propagation occurs as long as the separation is below $\lambda / 4$ [37]. By inserting a PEC narrow line inside the PMC surface, there will be a wave propagation along the PEC/PEC

line only, and there will be a complete stopband for the PEC-PMC plate. Fig. 2.5 illustrates the basic theory of gap waveguide.

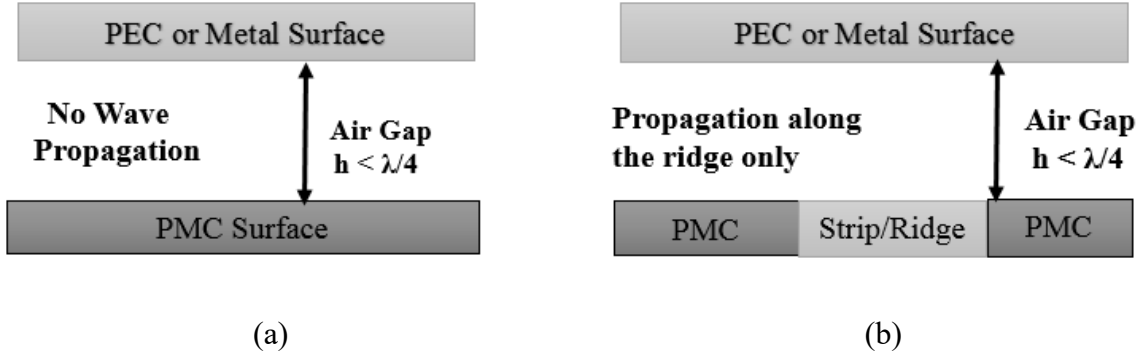


Figure 2.5: (a) PEC-PMC parallel plate, (b) Ridge surrounded by PEC/PMC surfaces.

Based on the above discussion, the structure with a bed of nails can create a high impedance surface, also known as AMC surface which stops wave propagation and the ridge will allow the wave propagation. This idea is known as Ridge Gap Waveguide, which will be discussed briefly in the next section.

2.3.4 Ridge Gap Waveguide

Ridge gap waveguide (RGW) is one of the promising guiding structure with a lower loss which could be suitable for higher frequency RF circuits and passive devices. RGW consists of two parallel plates, one plate with periodic textures to stop the wave propagation in all directions except the required path. There won't be any dielectric losses as it is a complete metal structure. In RGW there are no side walls as a rectangular waveguide. The metal RGW is illustrated in Fig. 2.6.

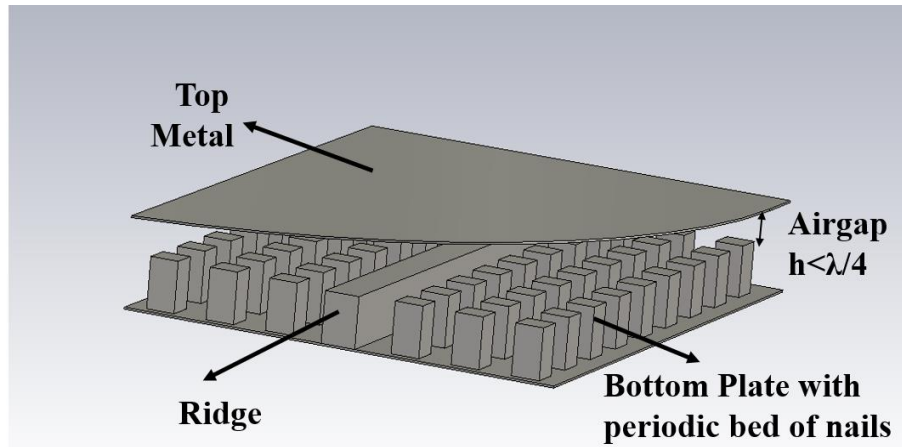


Figure 2.6: Ridge surrounded by bed of nails.

The bottom plate that contains the 2D periodic bed of nails controls the bandgap of the waveguide and the distance between the ridge, and the top metal should be less than $\lambda/4$. Due to low loss, and high power handling capability, it is considered among the promising mm-wave guiding structures and validated experimentally [38, 39].

2.3.5 Unit Cell Analysis

Artificial magnetic conductor (AMC) can be realized using the help of the bed of nails in both dimensions. The unit cell controls the bandgap and the operating bandwidth of the waveguide using the AMC surface. The bandgap of the unit cell is obtained from Eigenmode solver using CST Microwave Studio. Four important parameters play a significant role to change the stopband. Firstly, the air gap between the two conducting plates. Secondly, the height of the pin. Thirdly, the radius of the pin and finally, the pin to pin distance. The proposed design structure of a unit cell is illustrated in Fig. 2.7.

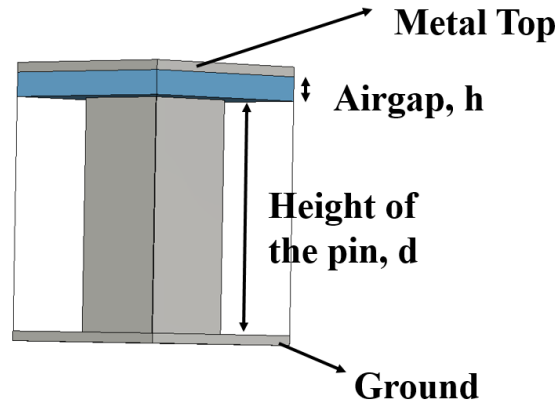


Figure 2.7: Unit Cell of a ridge gap waveguide structure.

Based on the requirement it is possible to choose the bandgap by changing these four parameters. For the bandwidth enhancement of the periodic structures, different shapes of periodic cells were analyzed to increase the realized bandgap [40].

2.4 Some other types of Gap Waveguides

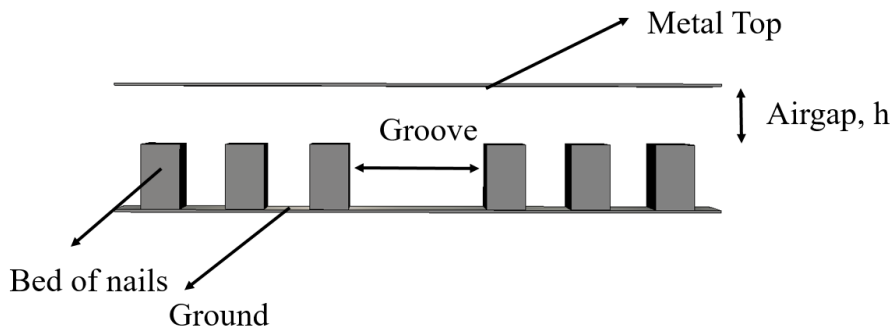
There are some other types of gap waveguides available. One of the most common is the groove gap waveguide. The other one is the inverted microstrip gap waveguide. We will discuss these two waveguides in the following section.

2.4.1 Groove Gap Waveguide

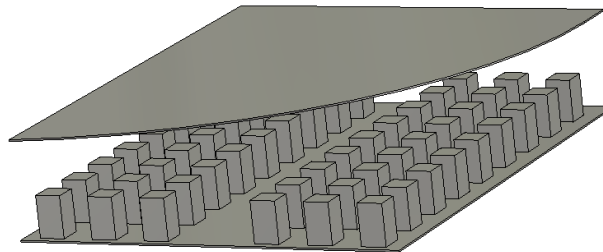
Groove gap waveguide is one of the most commonly used waveguides for mm-wave applications. In terms of losses and performance, it is better than even ridge gap waveguide.

In a groove gap waveguide, there is no ridge in the bottom plate. The ridge is replaced using a groove embedded with pins on both sides, which is shown in Fig. 2.8 (a). The difference between ridge and groove gap waveguide is that in groove gap it supports TE/TM modes [41, 42]. The dominant mode of groove gap waveguide is similar to the

dominant mode of a rectangular waveguide which is TE_{10} . On the contrary, ridge gap waveguide doesn't support TE/TM modes. Groove gap waveguide has fewer losses because it does not have any ridge and it has more volume for the current densities. The Q-factor of the groove is much higher than the ridge, which results in lower attenuation. In Fig 2.8(b) the complete structure of groove gap waveguide is shown.



(a)



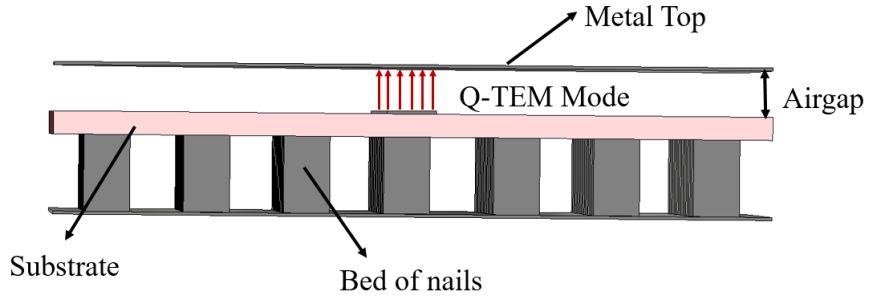
(b)

Figure 2.8: (a) Cross section of Groove gap waveguide. (b) 3D structure of Groove gap waveguide.

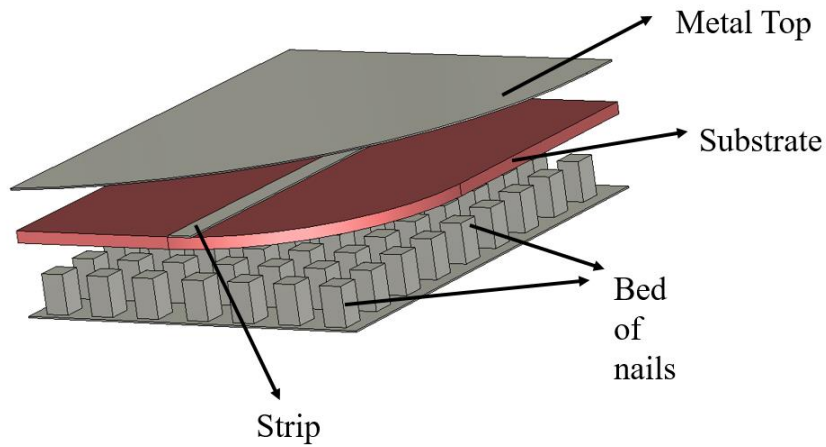
2.4.2 Inverted Micro-strip Gap Waveguide:

The desired mode in RGW, PRGW, and inverted micro-strip gap waveguide are similar [43]. The cross-section and the structure of the Inverted micro-strip gap waveguide are

shown in Fig. 2.9. Usually, in inverted microstrip gap waveguide, the microstrip is loaded on top of the bed of nails. Here the AMC forces the field to propagate in the air gap, between microstrip lines and the top metal.



(a)



(b)

Figure 2.9: (a) Cross section of Inverted Micro-strip Gap waveguide, (b) Complete structure of inverted micro-strip gap waveguide.

2.5 Ridge Gap Waveguide based Antenna

Gap waveguide is a low loss guiding structure which can work beyond 30 GHz and is a promising structure for the mm-wave application. RGW has no dielectric loss, as the signal propagates inside an air gap and it supports Q-TEM mode like a microstrip line. Recently

it has drawn a lot of attention, and a significant amount of research works had been already presented to improve the performance of the antenna based on gap waveguides.

The array of slot antennas has been widely using for radar and communication devices, where high gain is required. As slot antenna has a narrow bandwidth, so a lot of articles had been published to improve the bandwidth of this type of antennas. One possible solution is to deploy a T-junction at the end of the ridge and place a slot just on top of the T-shape ridge to widen the bandwidth [44]. Slot Antenna arrays with and without cavities used for the beam-scanning purpose, and it was highly directive [45-48]. Also, microwave components for the mm-wave and sub-mm-wave like filters, couplers, power dividers were analyzed using ridge gap waveguide [49-55]. Also, magneto electro dipole and superstrate was used to improve the bandwidth, and to reduce both the cross polarization and side lobes [56, 57]. In one work, 2-D scanning ME dipole was fed by RGW butler matrix, to form a beamforming network [58]. Fig 2.10 illustrates the structure of the ridge gap waveguide antenna. Many articles proposed a mixed technology between SIW and PRGW. The SIW cavity concept 2 x 2 and 4 x 2 slot element was used in upper PCB using SIW technology, which was excited by a coupling slot, the top metal of the PRGW structure [59, 60]. Other work has been presented to feed two leaky wave antennas out of phase for high gain based on modern guiding structures such as SIW and RGW [61]. Moreover, highly efficient unpackaged 60 GHz antenna array was designed for high gain purpose [62]. E-SIGW was introduced in for integrated horn antenna to use a thicker aperture than its planar feeding [63]. It gives more degree of freedom to shape the ridge without changing the unit cells.

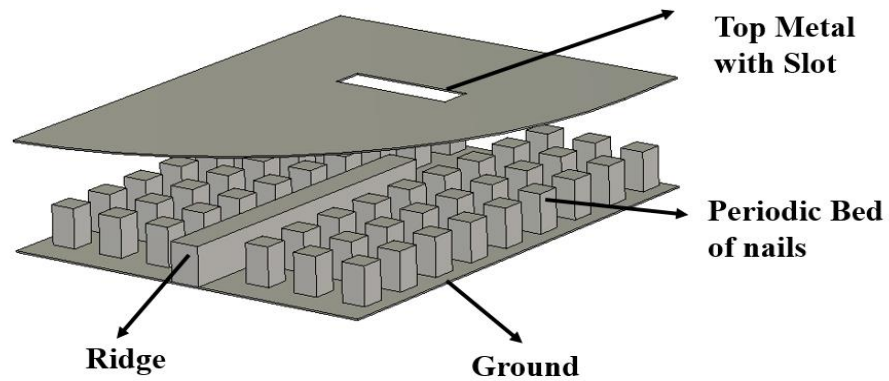


Figure 2.10: Metal Ridge Gap Waveguide Antenna.

2.6 Bow-tie Antenna

Bow-tie antenna is a dipole antenna which can provide wide bandwidth. Several techniques have been implemented to improve the bandwidth of the bow-tie antenna, in particular, flaring in the form of bi-conical structure is one of the conventional method [24]. The arms of the bow-tie antenna have a significant impact in increasing the bandwidth which is described in [23]. In our work, to increase the bandwidth of the antenna, we have utilized a bow-tie slot antenna on top of the ridge for wideband operation. A slot antenna is a complementary of a dipole antenna. If a slot is placed horizontally it will give vertical polarization and vice versa. However, for a dipole antenna a vertical dipole placed vertically will provide a vertical polarization. The impedance of the slot antenna can be calculated using the ‘Babinet’s Principle’ [23].

$$Z_d Z_s = \frac{\eta_0^2}{4} \dots\dots\dots (2)$$

Where, $Z_d =$ Dipole impedance, $73 + j42.5$,

$Z_s =$ Slot impedance,

$\eta_0 =$ Intrinsic impedance, 377Ω

All the values are in free-space.

A linear slot antenna is a resonant antenna and is solely dependent to the slot length. For a proper radiation the slot length has to be $\lambda/2$. A traditional slot will not provide more than 4-5 % bandwidth at the center frequency; however, using a bow-tie slot can offer higher bandwidth; thus it can improve the matching level. Because for bow-tie antenna the bandwidth depends on the angle and the length of the slot.

2.7 Summary

In this chapter, we have discussed and reviewed different kinds of antennas for mm-wave applications. At first, the low profile antennas for different applications with different techniques followed to enhance the antenna gain, bandwidth, and efficiency for mm-wave applications. Later we have described horn antenna, SIW based antenna and in the final section antennas based on RGW was described. The fundamental concept of RGW technology is described along with some other existing guiding structure which falls under the category of gap waveguides. Table 2.1 represents a summary of all the technologies in terms of the radiation pattern, gain, antenna shape, and losses.

Table 2.1 Comparison of different antenna configurations with different technology

Antenna Name	Radiation	Gain	Loss	Shape
Microstrip Antenna	Broadside and Endfire	Moderate	High	Planar
Horn Antennas	Broadside	High	Low	Bulky
SIW based Antenna	Endfire and Broadside	High	Moderate	Planar
PRGW	Broadside	High	Low	Planar

In the next chapters, we will cover the design methodology of the single element antenna, unit cell analysis along with the microstrip-ridge transition. Techniques to enhance the bandwidth and gain will be elaborately discussed in the next chapter along with the radiation patterns in E- & H- plane.

Proposed Single Element Bow-tie Slot Antenna with PRGW

3.1 Design Methodology

The concept of Printed ridge gap waveguide can be realised with periodic patches with plated vias which controls the bandgap of the structure. The design methodology of this proposed work is illustrated in Fig. 3.1.

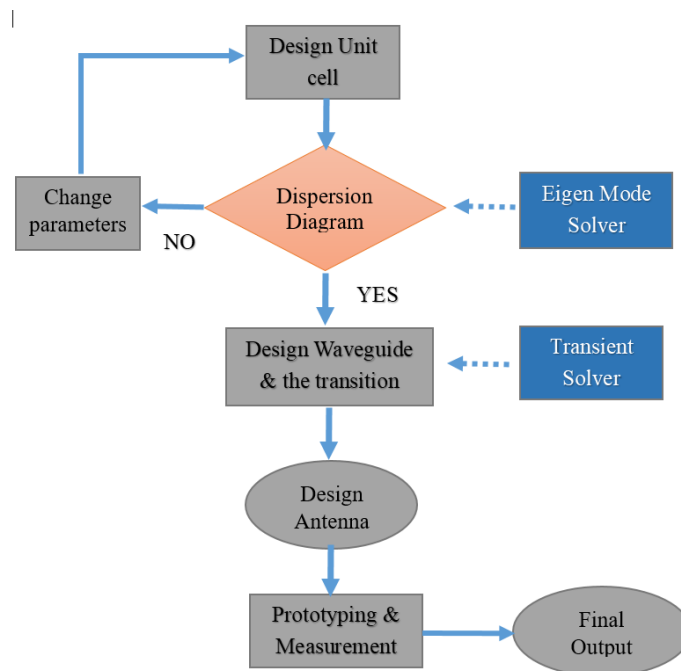


Figure 3.1: Flowchart of the proposed work.

The unit cell is the repetition of the same cells in 1D or 2D for a finite number of times. As a result of this periodic cells, a high surface impedance is observed in the bottom surface which does not allow the wave propagation. The unit cell for the proposed work is done

using Eigen Mode Solver (CST Microwave Studio), and the periodic boundary conditions are applied to get the result. Here it should be mentioned that in Eigen Mode solver there are no ports. It starts solving the problem from Maxwell's curl equations for both electric and magnetic field. Taking double curl in both these equations will individually give us the wave equation of electric and magnetic fields [23, 24]. From the wave equation the propagation constant, K can be calculated which will give us the dispersion diagram which depends mostly on the air gap of the ridge and the top metal. There are several other factors which will be discussed in the next sections. If we don't get the accepted bandgap, then we have to change the parameters to achieve the desired results. After obtaining the realized bandgap, the next step is to design the waveguide and the transition. For developing the waveguide the 'Transient Solver' is used which uses finite integration technique (FIT) to solve the problem and it applies the integral Maxwell's equation. For designing the PRGW, we have to apply the PEC boundary condition so that $E_{tan}=0$, and only the normal electric field exists. The H_{tan} produces a surface current due to the PEC boundary condition. The periodic patches act like an Artificial Magnetic Conductor (AMC) where there won't be any existence of normal electric field. The next part is designing the antenna using the transient solver. After the simulating results, the fabrication is done and after that the measurement we check and verify the final results.

3.2 Printed Ridge Gap Waveguide (PRGW)

The printed version of gap waveguides also known as the Printed Ridge Gap Waveguide (PRGW) is studied in terms of losses, bends and analyzed using microstrip ridge transitions [64, 65]. Later a fully PRGW was fabricated using a printed circuit board (PCB) technology

[66-68]. In this case, a mushroom patch is plated on top of a substrate and is connected to the ground plane by posts through vias which can provide the desired band gap. The capabilities of this new technique are promising since the structure is light and low cost and the performance regarding the loss is incomparably better than conventional micro-strip lines and SIW. The proposed structure for the PRGW is shown in Fig. 3.2.

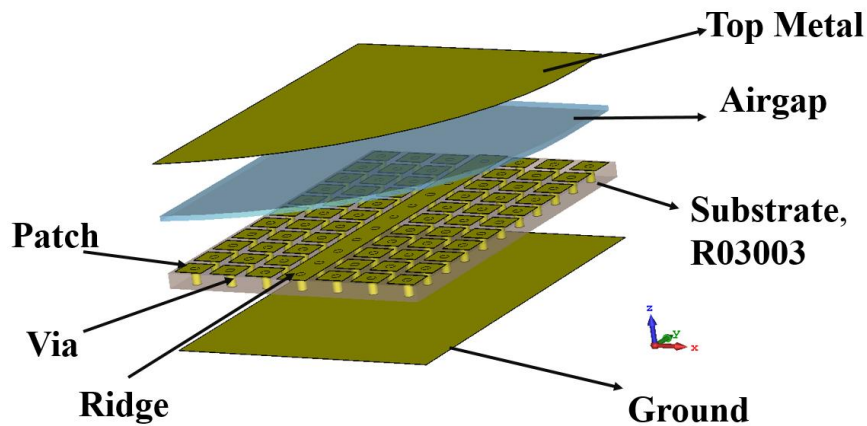


Figure 3.2: Proposed structure of the printed ridge gap waveguide.

Fig 3.3 illustrates the periodic unit cell with a ridge that is printed using Roger's 3003 substrates with $\epsilon_r=3$. Where, the dimensions of the ridge width, the width of the patch, radius of via, airgap, substrate thickness, and top metal thickness is 1.3mm, 1.2mm, 0.1875 mm, 0.253 mm, 0.75mm and 0.0175 mm respectively.

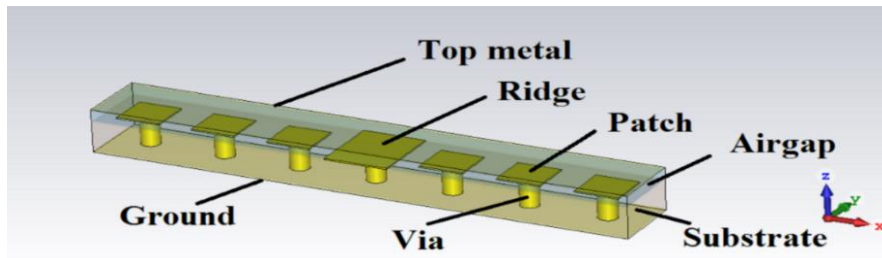


Figure 3.3: One row of unit cell with ridge

The proposed unit cell is designed to cover 24-45 GHz which is the operational bandwidth of the PRGW. In Fig. 3.4 the dispersion diagram with ridge is illustrated.

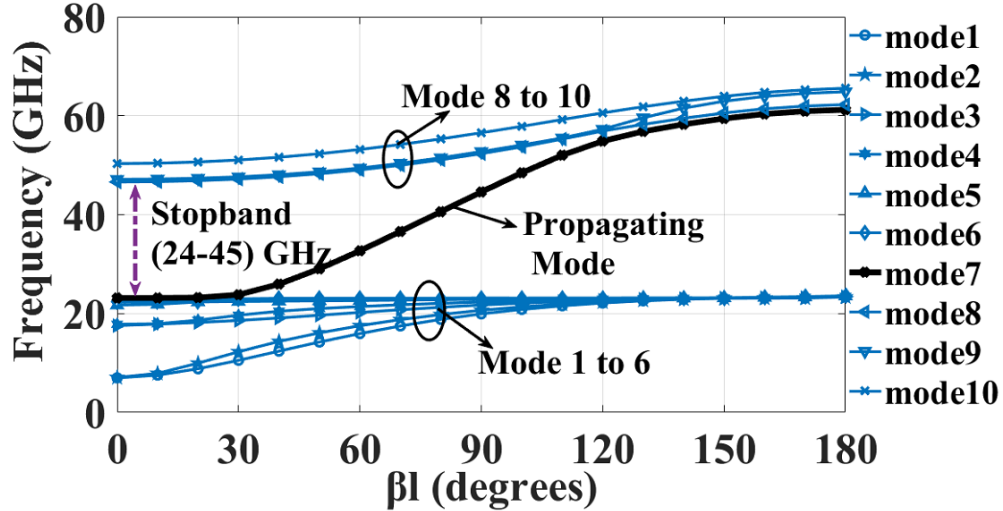


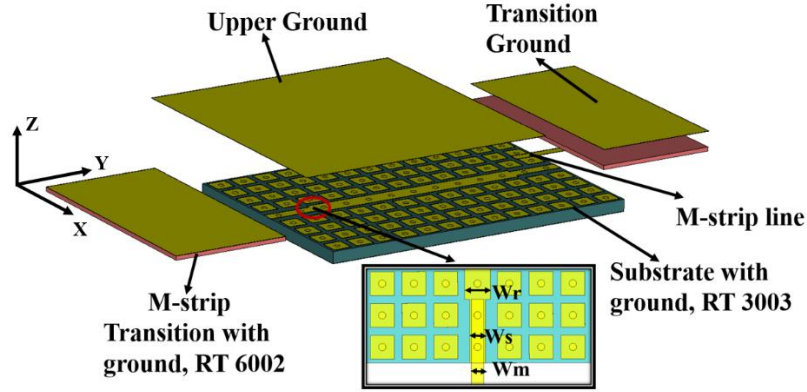
Figure 3.4: Dispersion diagram with the ridge existence.

From Fig. 3.4 it can be seen that there is a complete stopband from 24-45 GHz. In this range, only the wave will only propagate within the ridge. It can be referred to as realized bandgap as we are considering the ridge with one row of the unit cell.

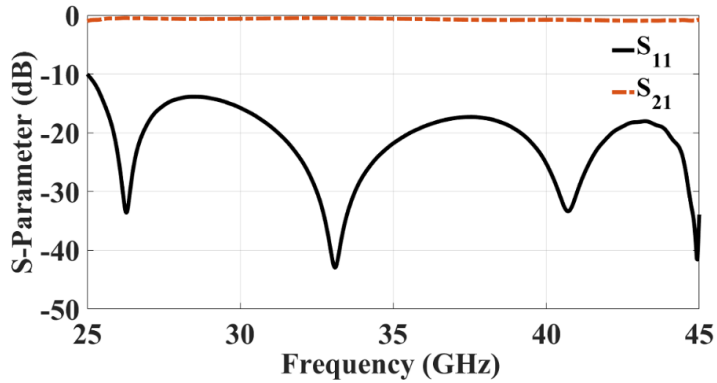
3.3 RGW Excitation

Ridge gap waveguide (RGW) is not a standard technology, which can be launched directly using standard measurement equipment; hence it is required to feed the waveguide with some standard transitions like coaxial transition, microstrip transition, etc. [67-70]. Many experimental setups are established to test the guiding structure. In our work, for feeding the PRGW, a Microstrip-ridge transition is considered which is illustrated in Fig. 3.5(a); for a clear illustration the ground of the microstrip line is hidden. The microstrip to ridge transition has already investigated in many published articles [65-67]. The S-parameter of the proposed microstrip-PRGW transition is illustrated in Fig. 3.5(b) and it is clear that the

transmission coefficient is close to -0.5 ± 0.2 dB in the whole operational bandwidth, which is due to the insertion losses from the input/output lines of the transition.



(a)



(b)

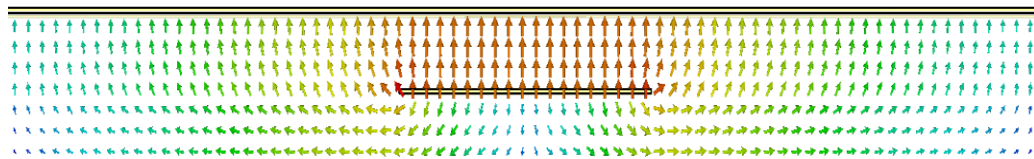
Figure 3.5: (a) Microstrip to Ridge Transition. (b) Simulated S-parameter of the PRGW transition.

The operational bandwidth of the waveguide is over (25-45) GHz which is similar to the realized bandgap of the proposed waveguide. At high-frequency bands, the performance of the microstrip line degrades as it suffers from cavity modes, which leads to surface waves. Due to the bending of the transmission line, there will be leakage and diffractions; as a result, most of the guided signals will lose its energy. This complication can be solved using PRGW where the wave only travels within the ridge, and the mushroom patches

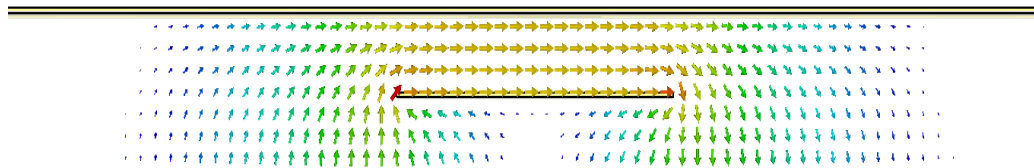
cancel the wave propagation transverse to the ridge direction so that we can minimize the leakage of transmission lines due to bending [65, 66].

3.4 Operating Modes of RGW

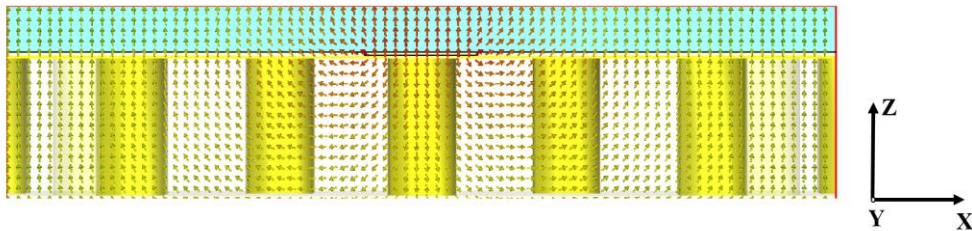
The mode of PRGW is similar to a microstrip line, which is quasi TEM or Q-TEM mode. Most of the waves confine within the dielectric substrate, and some parts are propagating in the air, so there will be a difference in phase velocities in two mediums which will create a Q-TEM mode, and in the edges of the microstrip lines, there will be some fringing fields. Fig 3.6 represents the port mode of the designed waveguide, and it is visible from the figure that the orientation of the ridge is in the Y direction, and PEC boundary condition is applied



(a)



(b)



(c)

Figure 3.6: Electric & Magnetic field distribution from the port end, (a) E-field (b) H-field, (c) E-field distribution from M-strip transition port end.

in the Z-axis, so for the ground plane and the ridge, only the normal electric field component will exist according to the PEC boundary conditions. In X & Y plane periodic boundary condition is applied which will act as a high impedance surface. For the proposed design from the port end, E_z is the normal electric field, which is perpendicular with the magnetic field H_x . E_z & H_x both are transverse to the direction of propagation which is orient in the Y direction. There are no exact formula to calculate the characteristics impedance of the ridge itself. Some numerical analysis was done to estimate the line impedance, which almost gave quite an accurate prediction [38]. One way is to do a full-wave simulation and after that to see the reference impedance.

3.5 Field Distribution along RGW

The periodically printed unit cells are used to cancel the field propagation transverse to the ridge direction. Theoretically, there won't be any fields propagating transverse to the ridge direction if we apply the magnetic boundary. However, there is no real magnetic surface in nature, so some field components transverse to the ridge direction will exist definitely. Fig. 3.7 illustrates the field distribution behavior of a periodic structure within a bandgap.

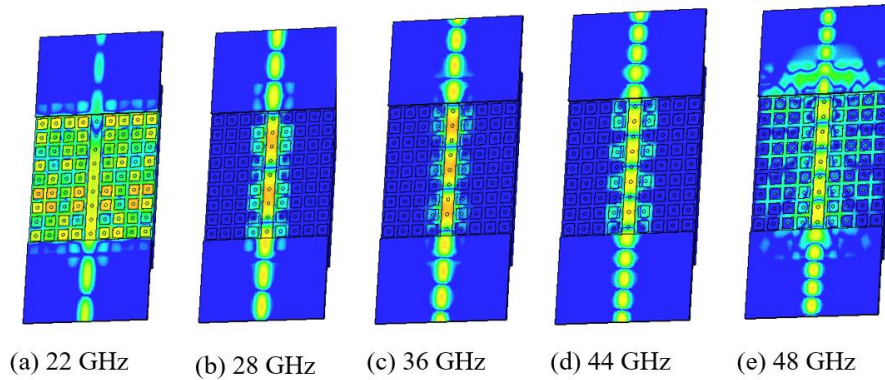


Figure 3.7: Field distribution of PRGW using microstrip transition at various frequencies.

From Fig. 3.7 it is evident that using PRGW as a guiding structure does not encounter cavity modes and surface waves within the operating bandwidth of the waveguide over 24-45 GHz, which is very common for microstrip lines at high frequencies. Hence within the stopband, the EM wave is guided properly along the ridge. Thus, before and after this stopband the fields get scattered and it degrades the overall power transfer from one port to another, as the transmission coefficient decreases dramatically. After three columns of mushroom patches both sides from the ridge, the field strength gets very weak and it becomes almost zero. Even if there is a bend in the ridge, it does not affect the overall power transfer of the PRGW, which makes it suitable for developing power dividers, couplers, and other microwave components.

3.6 Applications of RGW

RGW has already gained its prominence and becoming very attractive in modern & future wireless communication systems. The application of RGW is not only limited as a guiding structure, but it can also integrate with Monolithic microwave integrated circuits (MMICs) and packaging devices. Several microwave circuits like couplers, filters, power dividers were designed based on this technology which is discussed already in details in chapter 2. Beamforming network components, such as couplers, crossovers, butler matrixes are designed based on this promising technology [71]. Besides, beamforming antennas for scanning & steering purpose have developed recently. Some other works such as textile material characterizations with straight RGW is also established using this technology [72]. Recently, the reconfiguration feature is implemented namely, reconfigurable printed ridge gap waveguide technology (RPRGW) [73, 74]. This technology enables the

implementation of reconfigurable microwave components needed for the construction of robust and adaptable communication systems.

3.7 Printed Ridge Gap Waveguide Antenna

Printed ridge gap waveguide antenna (PRGW) is the printed version of ridge gap waveguide. It is built on a dielectric substrate, and the propagating medium is air so, there are no dielectric losses like microstrip lines or coplanar waveguides. It's a low profile antenna, which can give a broadside radiation pattern. A lot of works had been already done to enhance the gain and the operating bandwidth of the antenna and other microwave components which had been previously covered in the literature review section [32-49].

3.7.1 PRGW Antenna using linear slot

PRGW is a packaged structure, so for the antenna to radiate the above ground is etched or cut for the radiation. At first, a simple vertically polarised slot is designed to provide broadside radiation. The proposed antenna with a linear slot is shown in Fig. 3.8.

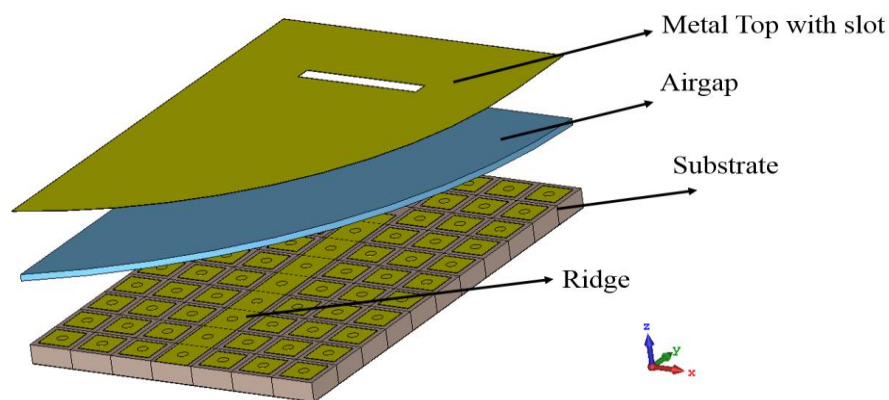


Figure 3.8: PRGW antenna with linear slot.

Here the slot dimensions of the designed antenna are (4.7mm x 0.5mm) at 30 GHz. Fig. 3.9 illustrates the reflection coefficient of the design slot antenna and only 5.8 % impedance bandwidth is obtained using the linear slot at the center frequency from (29-30.8) GHz.

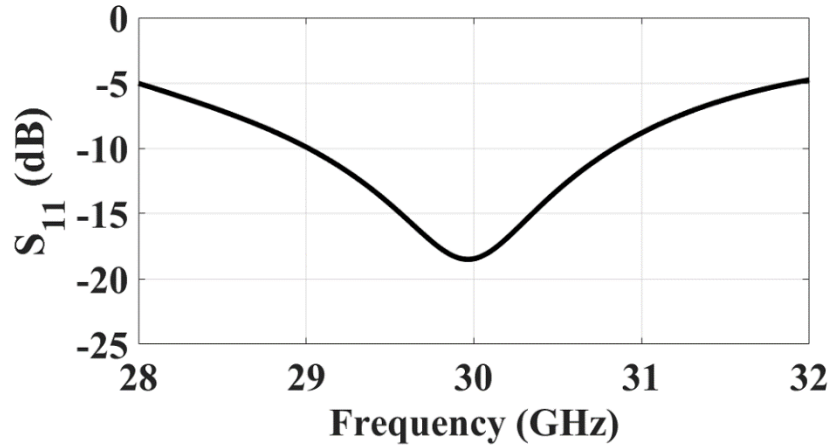


Figure 3.9: Reflection coefficient of the simulated slot antenna using PRGW.

3.7.2 T-shape Ridge along with multi-section transformers

To increase the bandwidth of the PRGW antenna a T-shape ridge was added at the end of the ridge. Generally, the slot is placed on top of the T-shaped ridge so that, there will be one resonance from the slot and another resonance from the T-shaped ridge itself. This idea was already deployed to provide a wider bandwidth [44]. The designed structure is illustrated in Fig. 3.10 and with this design, an impedance bandwidth of 14.6% is achieved. The length of the slot must be larger than the T-shaped ridges length, T_L so that wide bandwidth can be obtained. Multi-section transformers are used in microwave components and devices to get a wide bandwidth. Slot antenna itself has a narrow bandwidth, so by adding multi-section transformers both the bandwidth and matching level can improve significantly. In our design, a two-section Chebyshev transformer with T-shape ridge is deployed to obtain higher impedance bandwidth.

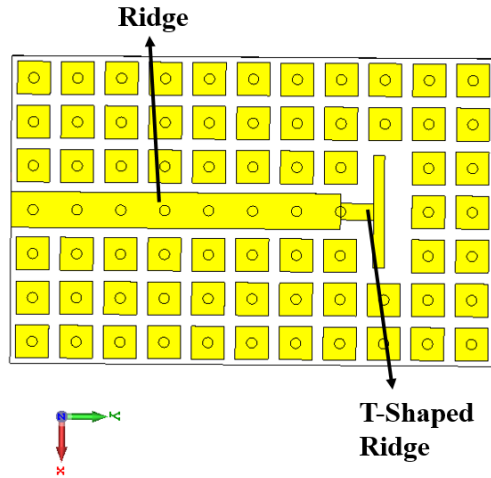


Figure 3.10: PRGW slot antenna with a T-shape ridge.

After adding the two-section Chebyshev transformers, the bandwidth improved significantly which can be clearly seen from the reflection coefficient. 18.5 % impedance bandwidth is achieved from (28.9-35) GHz, which is illustrated in Fig. 3.11.

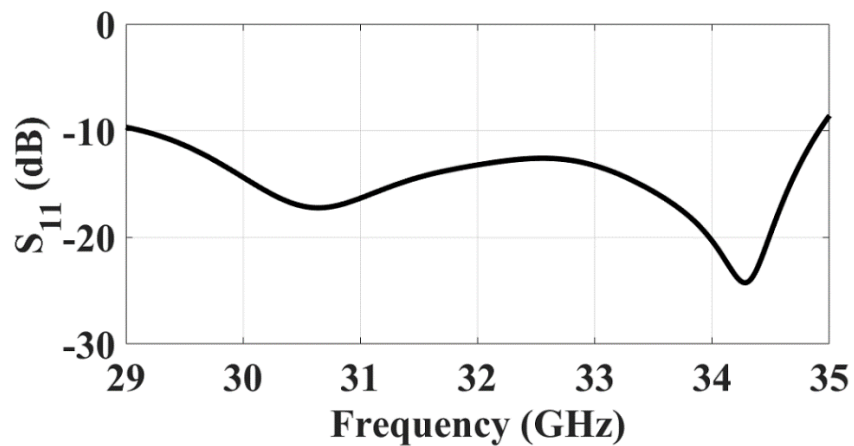


Figure 3.11: Reflection coefficient of two section T-shape ridge with PRGW.

3.8 Bow-tie Slot Antenna with Two-section T-shaped Ridge

In our work, a two-section T-shaped ridge with a bowtie slot is used to get higher bandwidth. A lot of techniques had been applied to improve the bandwidth of the antenna,

and for high data transmission, a wide bandwidth is mandatory. A linear slot with ridge gives only 4-5 % impedance bandwidth. Bow-tie antenna gives more impedance bandwidth than the traditional slot. The arms of the bow-tie have a more significant impact on enhancing the bandwidth level. The ratio of the slot length, SL and the T-sections length, TL has some effect on the bandwidth. For our design, we have considered the SL/TL ratio to be 1.6. A lot of parametric studies to choose the best value of TL were done as the bandwidth depends a lot on the TL, it is worth mentioning that the width of the T-section, TW does not have a substantial impact in widening the bandwidth. The proposed 3D structure of the single element antenna is illustrated in Fig. 3.12. To support the antenna structure and to keep the air gap thickness fixed a substrate, Rogers 6002 with 0.254 mm thickness on top of the bow-tie slot is placed to hold the antenna.

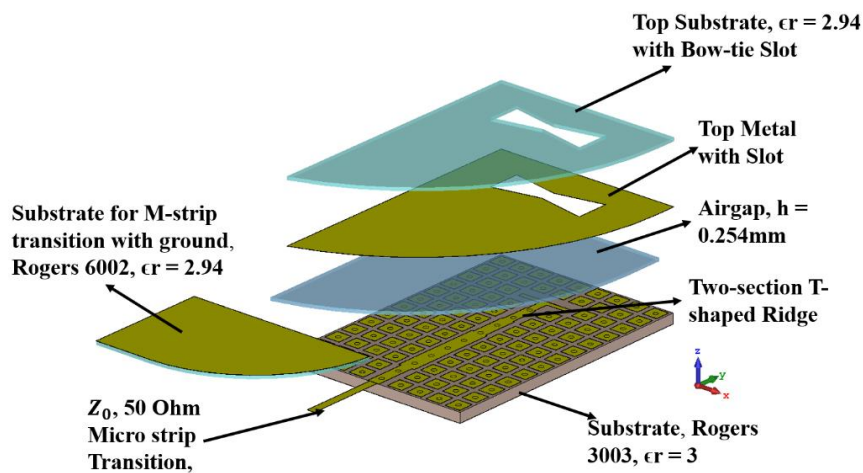


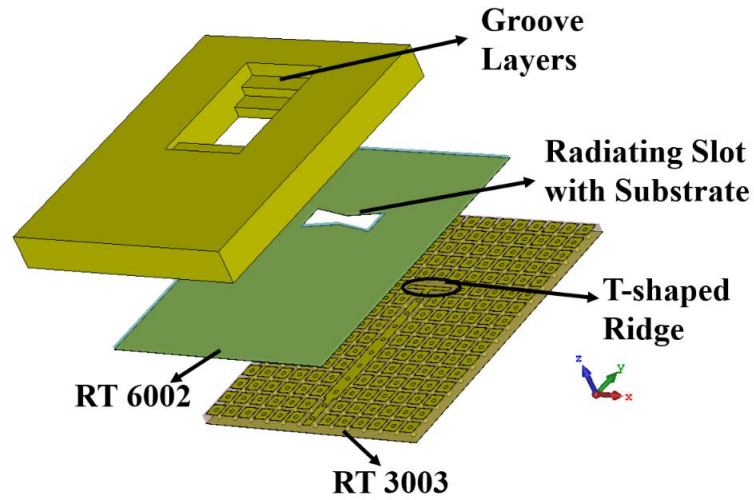
Figure 3.12: 3-D structure of a two section T-shaped ridge based on PRGW.

In the next section, we will discuss the three-layer, horn-like groove structure on top of the bow-tie antenna, and the reflection coefficient and gain compared with the single element antenna and the horn-like groove antenna will be explained using PRGW.

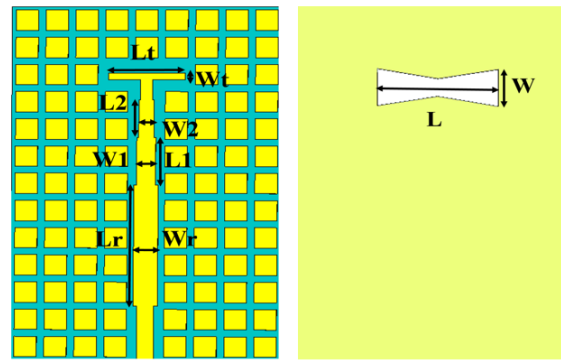
3.9 Three-layer Horn-like Groove Antenna with Bow-tie Slot

Here a two-section T-shaped ridge with a bow-tie slot is used to provide higher bandwidth.

The proposed single element antenna is shown in Fig. 3.13

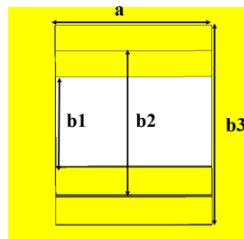


(a)



(b)

(c)



(d)

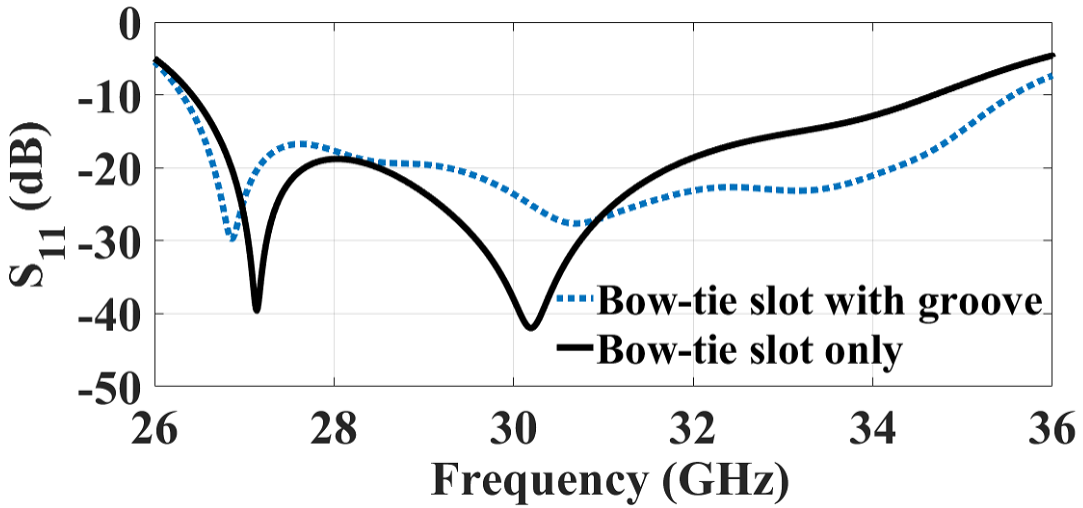
Figure 3.13: (a) Proposed 3D model for the single element bow-tie groove. (b) Feeding layer. (c) Bow-tie slot antenna layer. (d) Horn-like groove layer.

Table 3.1: Designed parameters for the proposed PRGW Antenna

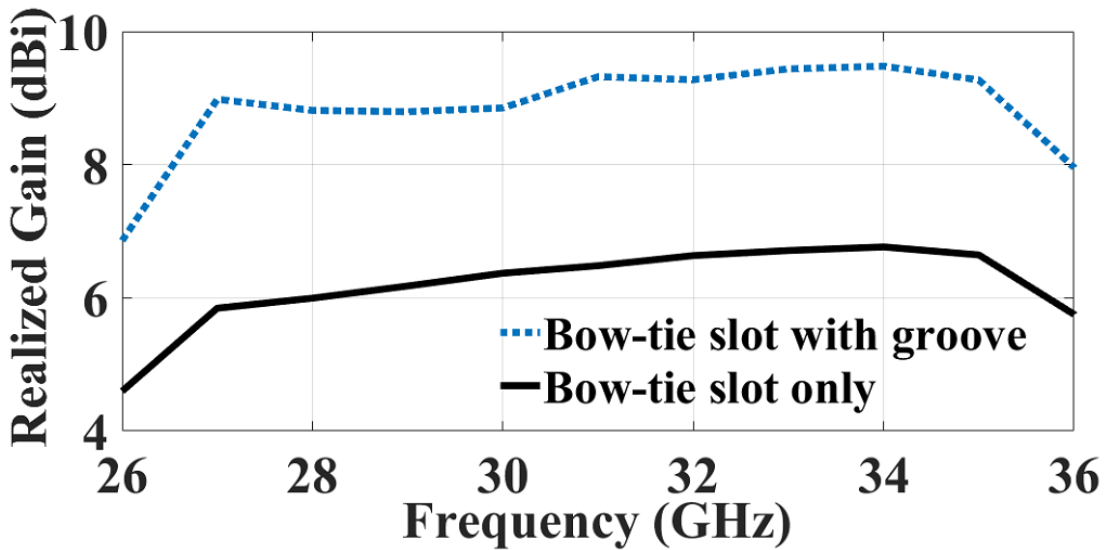
Designed Parameter	Value (mm)	Designed Parameter	Value (mm)
1 st Section length, L1	2.8	Groove width, layer 1, b1	5
1 st Section width, W1	1.015	Groove width, layer 2, b2	8
2 nd Section length, L2	2.2	Groove width, layer 3, b3	11
2 nd Section width, W2	0.81	Groove length, a	7.5
T-shaped length, TL	4.1	Slot length, L	6.4
T-shaped width, TW	0.4	Slot width, W	2.6
Width of Ridge, Wr	1.3	Length of ridge, Lr	7.8
Width of strip line, Ws	0.75	Airgap, h	0.254
Width of M-line, Wm	0.62	Groove depth	4.5

The single element PRGW antenna consists of three layers, the first one is the ridge with periodic cells, and the second layer is the bow-tie antenna printed on the Rogers RO6002 substrate. Finally, to increase the gain furthermore, a three-layer groove structure on top of the bow-tie slot is deployed where all layers have a total thickness of 4.5 mm. Here the groove dimensions were only increased in one axis, as shown in Fig. 3.13(d). The transition layer is not demonstrated as we have illustrated the microstrip-PRGW transition. The transition layer is only required while calculating the measurement results. The simulated reflection coefficient for the single element antenna with and without the horn-like groove structure is illustrated in Fig. 3.14(a). It is observed using groove layers enhanced the antenna bandwidth of up to 30.6 % from (26.3-35.6). Fig. 3.14(b) illustrates the gain versus frequency curve for both the antennas. It is very clear from the gain versus frequency curve

that, the gain is increased by 3 dB over the whole frequency range from (26-36) GHz after adding the groove layer. Table 3.1 shows all the proper dimensions of the design parameters. For this work, we have preferred to work at higher frequencies, above 30 GHz which is suitable for Space research service (SRS) & Radio astronomy service applications where the band allocation for this range is from (31.8-33.4) GHz.



(a)



(b)

Figure 3.14: (a) Simulated reflection coefficient of single element PRGW antenna. (b) Gain versus frequency for the single element antenna.

Besides, the E- and H-plane radiation patterns for the proposed antenna with and without the horn-like groove structure are shown in Fig. 3.15 at the center operating frequency. From the figure, it can be depicted using the groove layer the beam in the E-plane became narrower and a high gain is obtained. On the other hand, this groove structure keeps the antenna with low profile characteristics as the design is packed by the grooved metallic sheet that increases the gain and provides mechanical support.

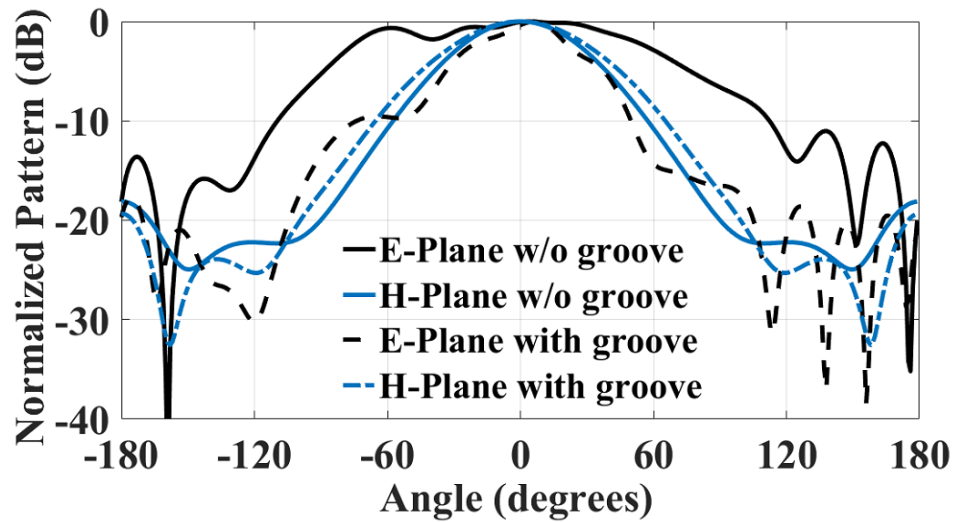


Figure 3.15: Simulated radiation pattern comparison for single element antenna at 30 GHz.

We have preferred a step-shaped aperture for our design as it's a cost-effective technique that can be realized using our fabrication facilities. The three-layer groove structure is fabricated in our fabrication lab with the milling machine. For making the surface like slope needs a higher accuracy fabrication process which leads to higher fabrication cost. To avoid this, we have preferred to increase the groove dimension layer by layer to simulate the sloping surface, where the groove can be fabricated using a low-cost machining facility. In our work, for the three-layer groove section, the dimensions in the H-plane are kept constant, and in the E-plane, the dimensions vary in a stepped size, which resulted in an

overall increase in the aperture area that provides a higher gain. Some parametric studies were done to choose the optimum value for this design which is shown in Fig. 3.16.

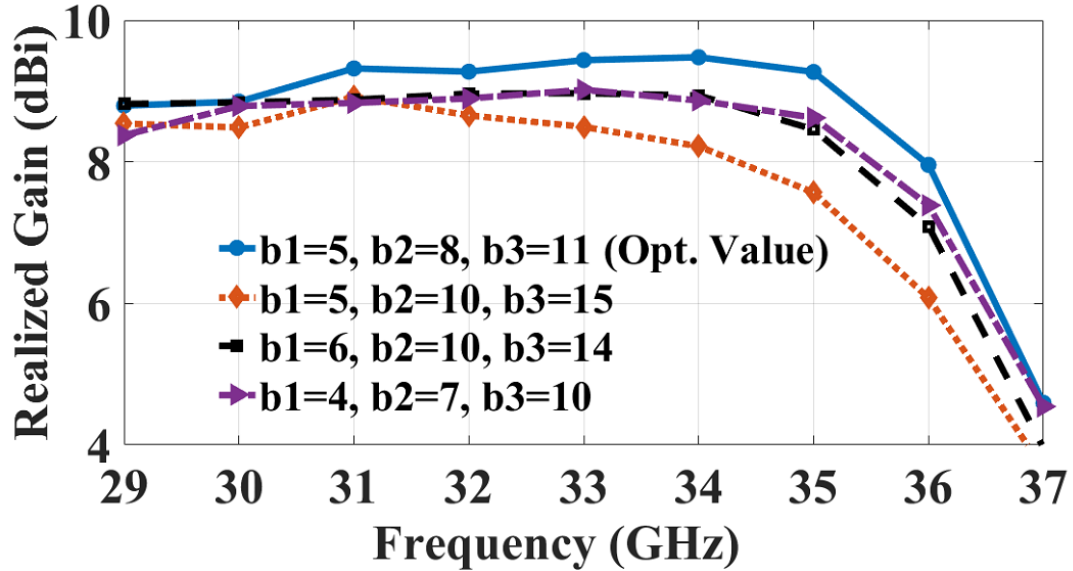


Figure 3.16: Simulated gain comparison by changing groove size.

In the next section, we will show a bow-tie shaped ridge with a bow-tie slot on top for wideband and high gain applications for mm-wave frequency bands.

3.10 Bow-tie shaped Ridge Slot Antenna Augmented with Superstrate

In this section, we propose a bow-tie shaped ridge with a slot antenna for a wideband and high gain application. A traditional linear slot can provide only 4-5 % bandwidth, which is not enough for high data transmission and high-speed connectivity. To get more bandwidth, we have proposed a bow-tie shaped ridge with bow-tie slot. Table 3.2 shows the proposed antenna with all the designed parameters and Fig. 3.17 illustrates the PRGW antenna with a superstrate.

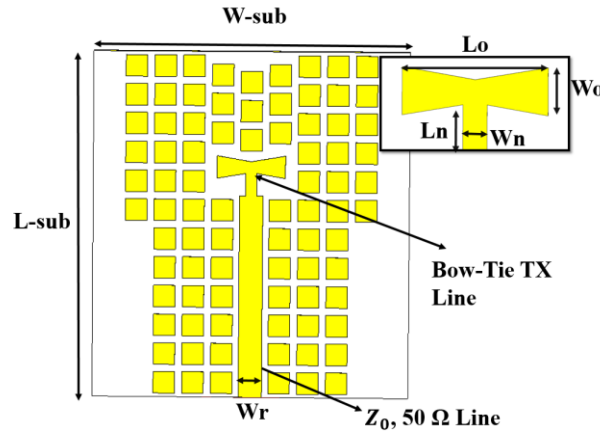


Figure 3.17: Proposed design of bow-tie shaped ridge along with parameters.

Table 3.2: Dimensions of PRGW Bow-tie Tx-Line with Slot Antenna (in mm)

Parameter	Value	Parameter	Value
L-Sub	19.2	W-sub	17.6
L _o	4	W _o	1.5
L _n	1.2	W _n	0.63
Ridge length, L _r	11.2	Ridge width, W _r	1.3
Slot length	5.6	Slot width	2.5

This design led to an impedance bandwidth of 12.3 % from (29-32.7) GHz. The slot is placed with a substrate so that, it can provide strong support to the overall structure. The ratio of the bow-tie shaped ridge with the slot length is kept 1: 1.4 and width is held 1:1.75 to get best possible bandwidth. Using a thin substrate instead of a thick one is wise as the thicker substrate will lead to more surface waves, which is not desirable. Later, to increase the bandwidth and gain of the antenna a superstrate is loaded at a distance of $\lambda/2$ which is centered at 30 GHz as shown in Fig. 3.18.

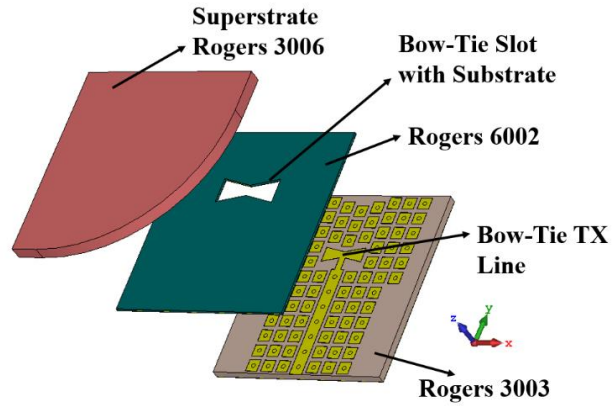
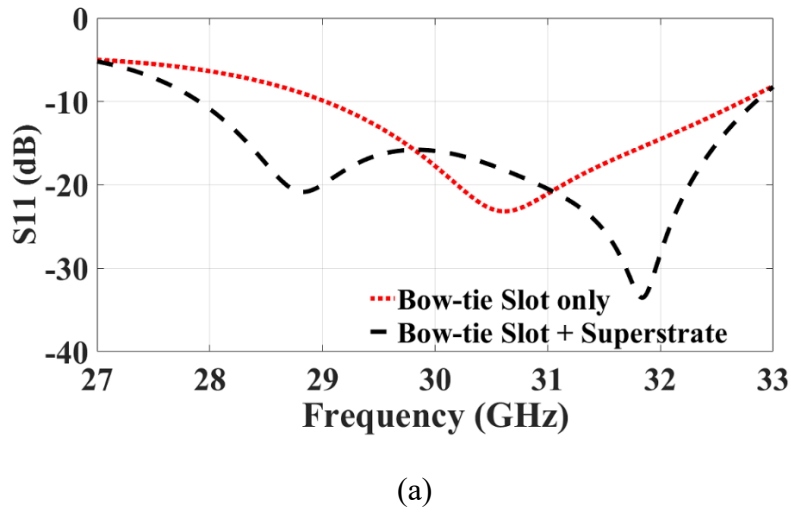
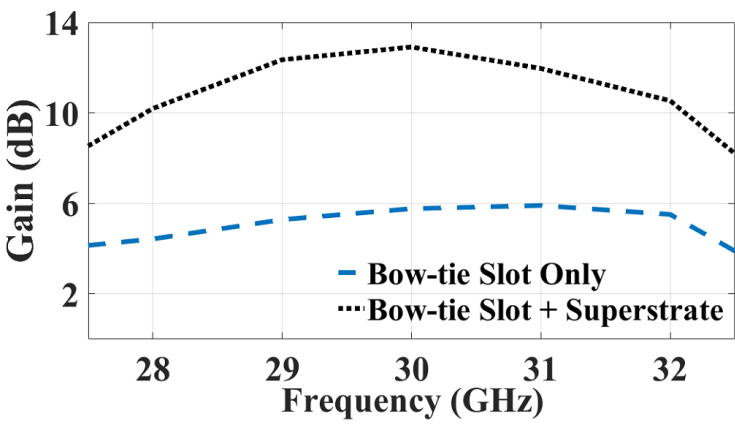


Figure 3.18: Proposed bow-tie slot antenna with superstrate.



(a)



(b)

Figure 3.19: (a) Simulated reflection coefficient of bow-tie slot antenna. (b) Gain versus frequency with and without the superstrate.

Fig. 3.19 illustrates the reflection coefficient and the gain versus frequency curve, and it shows clearly that the impedance bandwidth increased up to 16.8% from (27.9-32.8) GHz and after adding the superstrate and the gain increased up to 13 dB at the center frequency. This kind of antennas are suitable for high gain and wideband applications. In the next chapter, we will cover the feeding network based on PRGW technology. A novel 1 x 4 groove antenna array on top of the 1 x 4 slot antenna array is proposed to give a high gain up to 16 dB which will be along with the measurement results.

Chapter 4

Proposed Bow-tie Slot Antenna Array Based on PRGW

4.1 Feeding Network based on PRGW technology

For radar systems, satellite communication phased arrays, and integrated circuits arrays are used mostly where the inter-element spacing for fixed beam arrays is usually selected to be less than a free space wavelength (λ) [23, 24]. Low-profile single antenna element can't provide more than 10 dB gain. As a result, low profile, and planar structure microstrip arrays are used to achieve high gain. At mm-wave range designing microstrip arrays can be challenging because of the high dielectric losses at higher frequencies. In this work, the feeding network is constructed based on Printed Ridge Gap Waveguide (PRGW). Although, the power dividers and antennas are built with a PCB still there won't be any dielectric losses, because the propagating medium is air for the two parallel conducting plates. There are few possible ways to enhance the gain of the antenna, they are (i) Increasing aperture area (ii) Using superstrate or FSS structure and (iii) Designing Array antenna. It is not feasible to increase the aperture area, as it makes the overall structure bulky, which might not be suitable for all applications.

On the other hand, using superstrate or meta-materials can be complicated to build, while designing array is not complicated, and it can be developed easily and integrated. Microstrip array suffers from high dielectric losses and surface waves at higher frequencies. On the other hand, periodic structures like mushroom patches with plated vias, allows certain frequency bands to propagate and stops wave propagation for different

modes which create a bandgap. In this work, a 1 x 4 Bow-tie slot antenna based on PRGW technology has been proposed which we will discuss in the next sections.

4.2 Power divider based on PRGW

Ideally, a slot antenna can give 6-7 dB gain, hence for gain enhancement the utilization of array antennas are required. The feeding lines and the mushroom cells are print on the same substrate. Due to some of the bending's in the feeding lines and also in the quarter wave section, some of the periodic cells had to be relocated and moving a few cells do not have a significant impact on the results. It is worth mentioning that the periodic cells must be very close to the ridge and where there is a bending of lines.

4.2.1 1 x 4 Power divider based on PRGW

In this section, we propose the design of 1 x 4 Bow-tie slot antenna array using a PRGW technology and initially, a 1×2 feeding network is designed with a comparable level < -15 dB over (29-37) GHz. Then, a 1×4 power divider is constructed using the two-way feeding network, where the schematic view shows in Fig. 4.1(a) with all the required designed parameters. Fig 4.1 (b) represents the S-parameter of 1×4 power divider where the comparable level is below -15 dB in the required frequency band. The transmission coefficient to each port is around -6.5 dB over (29-37) GHz. It is possible to design the feeding network and EBG mushroom cells in two different substrates, which gives more degree of freedom to develop the feeding network. However, it will have one more extra layer of a substrate, to avoid that in our work the feeding lines and bed of mushrooms were printed in the same substrate.

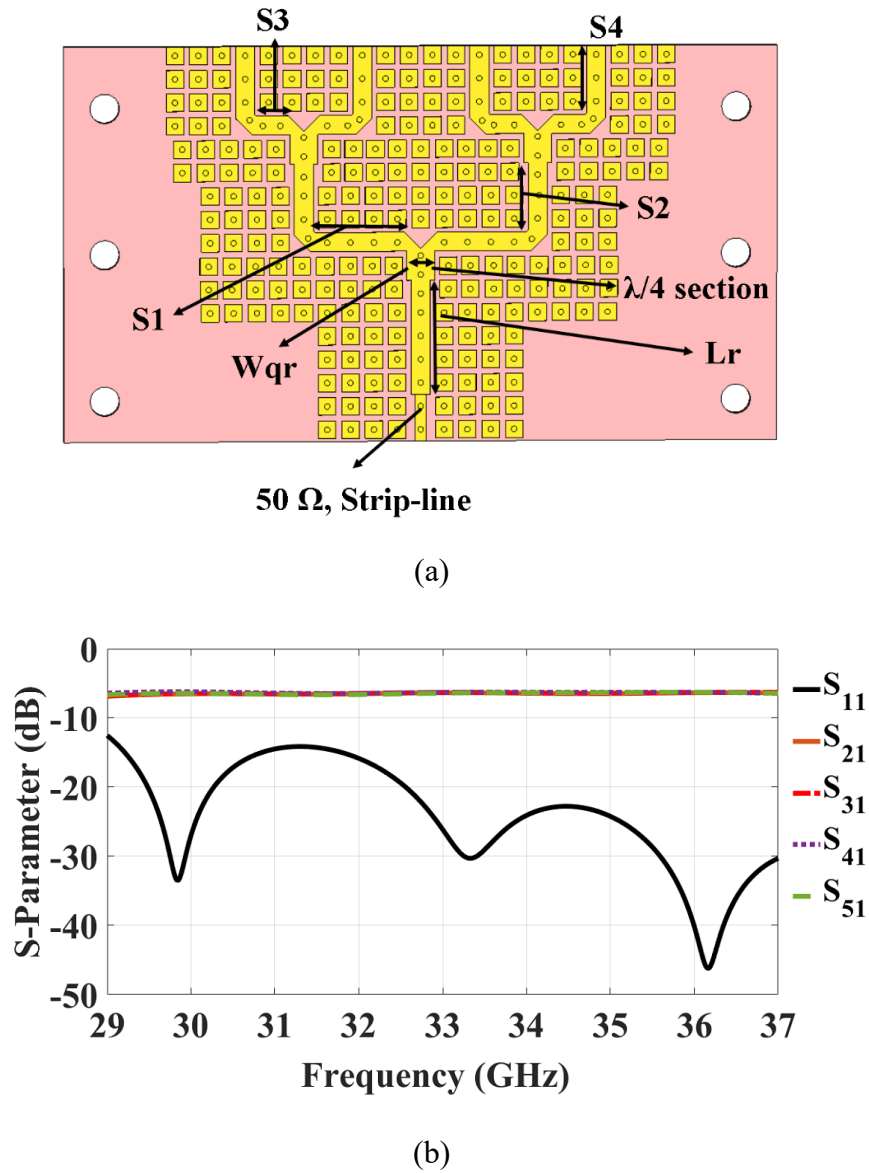


Figure 4.1: (a) Layout of 1 x 4 power divider. (b) S-parameter of the power divider.

4.2.2 E-field distribution of 1 x 4 Power divider based on PRGW

The E-field distribution of the proposed PRGW at 30 GHz is shown in Fig. 4.2 and it is demonstrated using 3-4 columns of periodic cells in between the two lines can eliminate the mutual couplings between the elements.

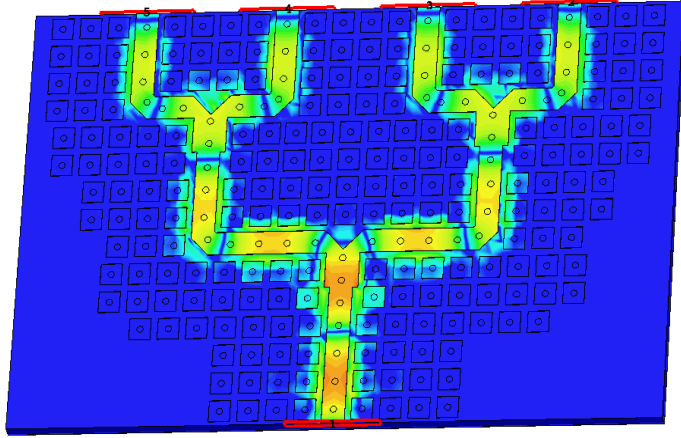


Figure 4.2: E- field distribution of 1 x 4 power divider using PRGW at 30 GHz.

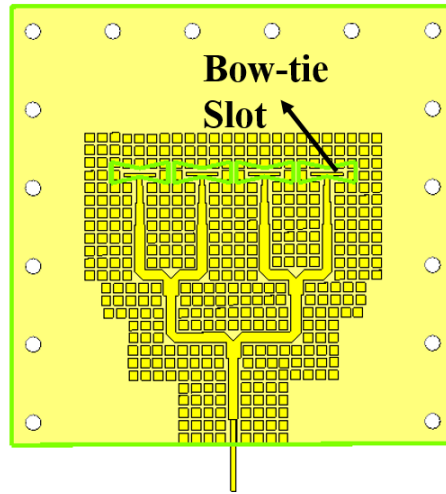
From Fig. 4.2, it can be depicted that the electric fields are confined mostly within the ridge at 30 GHz. The periodic cells are blocking the unwanted radiation caused the bending of the lines. With this new PCB guiding structure it is possible to suppress the unwanted radiation, which improves the overall power transfer from one port to another port.

4.3 1 x 4 Bow-tie Slot Antenna Array based on PRGW

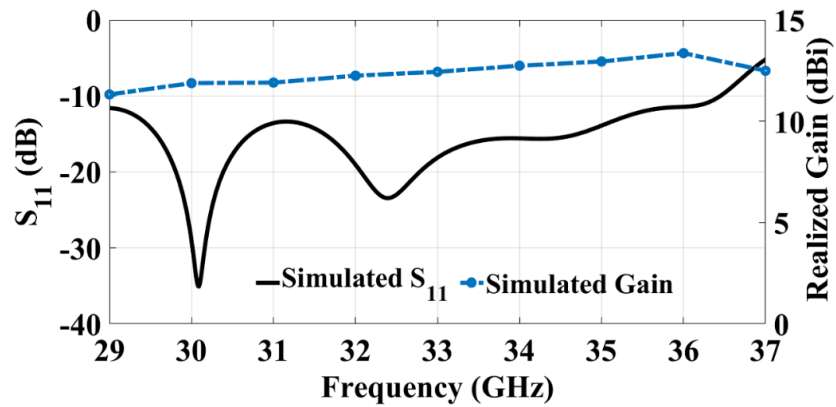
The designed 1 x 4 power divider is deployed to feed four bow-tie slot antenna elements as illustrated in Fig. 4.3 (a), where the reflection coefficient of the proposed array is shown in Fig. 4.3(b). It can be depicted that the proposed array structure gives a broad bandwidth of 23 %. The element to element spacing of the slot antenna is kept $0.8 \lambda_0$ where λ_0 is the free space wavelength at 30 GHz to avoid the grating lobes. Table 4.1 describes the dimensions of the quarter wave sections length and width along with the arms of the T-junctions.

Table 4.1: Dimensions of PRGW antenna array (in mm)

Parameter	Value	Parameter	Value
Lqr	2.3	Wqr	1.9
S1	8.65	S2	4.9
S3	4.65	S4	5.8
Lg	32	Wg	14



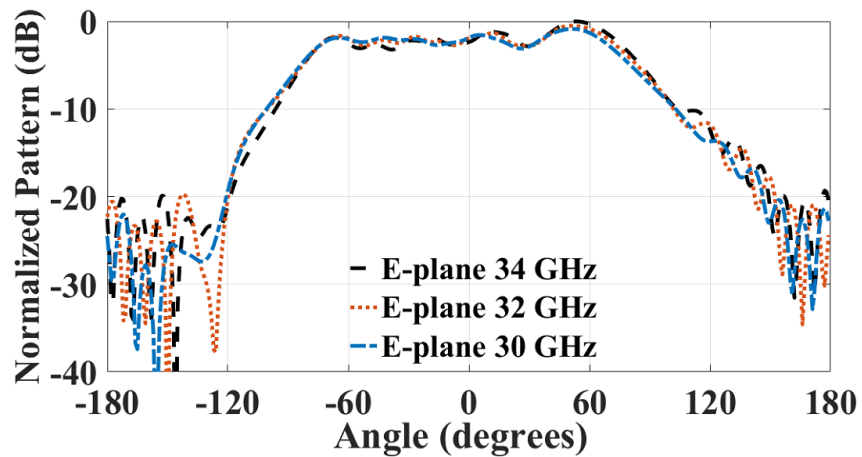
(a)



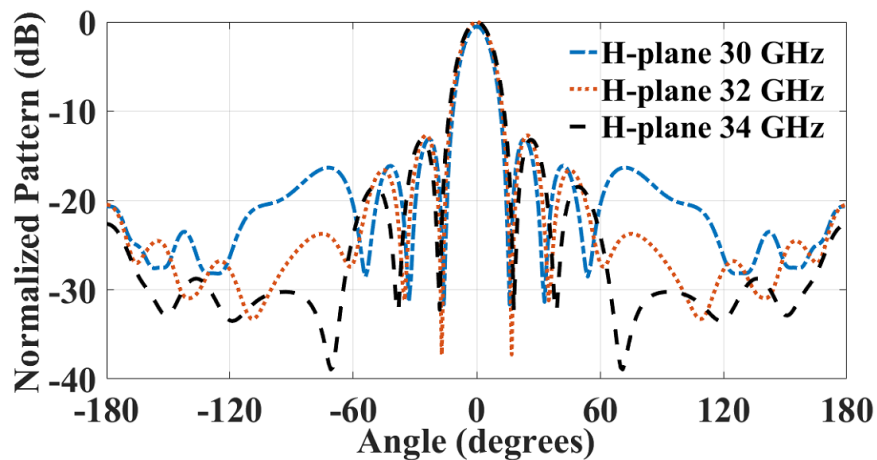
(b)

Figure 4.3: (a) Simulated model top view of the bow-tie slot antenna array. (b) Simulated reflection coefficient and gain of 1×4 bow-tie antenna array.

The radiation pattern of 1×4 Bow-tie slot antenna array is shown in Fig. 4.4 for the E- and H-plane at 30, 32 and 34 GHz. It shows clearly that the side-lobe level (SLL) is less than -13 dB with a steady gain as shown in Fig 4.3(b) throughout the whole frequency range over (29-37) GHz. The proposed antenna array has a narrow beam in the H-plane due to the four-element array and a wide beam in the E-plane mainly due to the element pattern. As a result, the beam is far-reaching in one plane compared to the other plane.



(a)



(b)

Figure 4.4: Simulated normalized radiation pattern for 1×4 bow-tie antenna array (a) E-plane, (b) H-plane.

4.4 1 x 4 Groove Antenna Array with Corrugation ring:

In this work, we have proposed a three-layer groove antenna array which is loaded on top of the designed bow-tie slot antenna array. Our primary objective of this work is to offer an antenna with high gain and higher bandwidth so that it can fulfill the requirement of mm-wave communication. Fig. 4.5(a) illustrates the proposed 1×4 groove antenna array and Fig. 4.5(b) shows the reflection coefficient & gain.

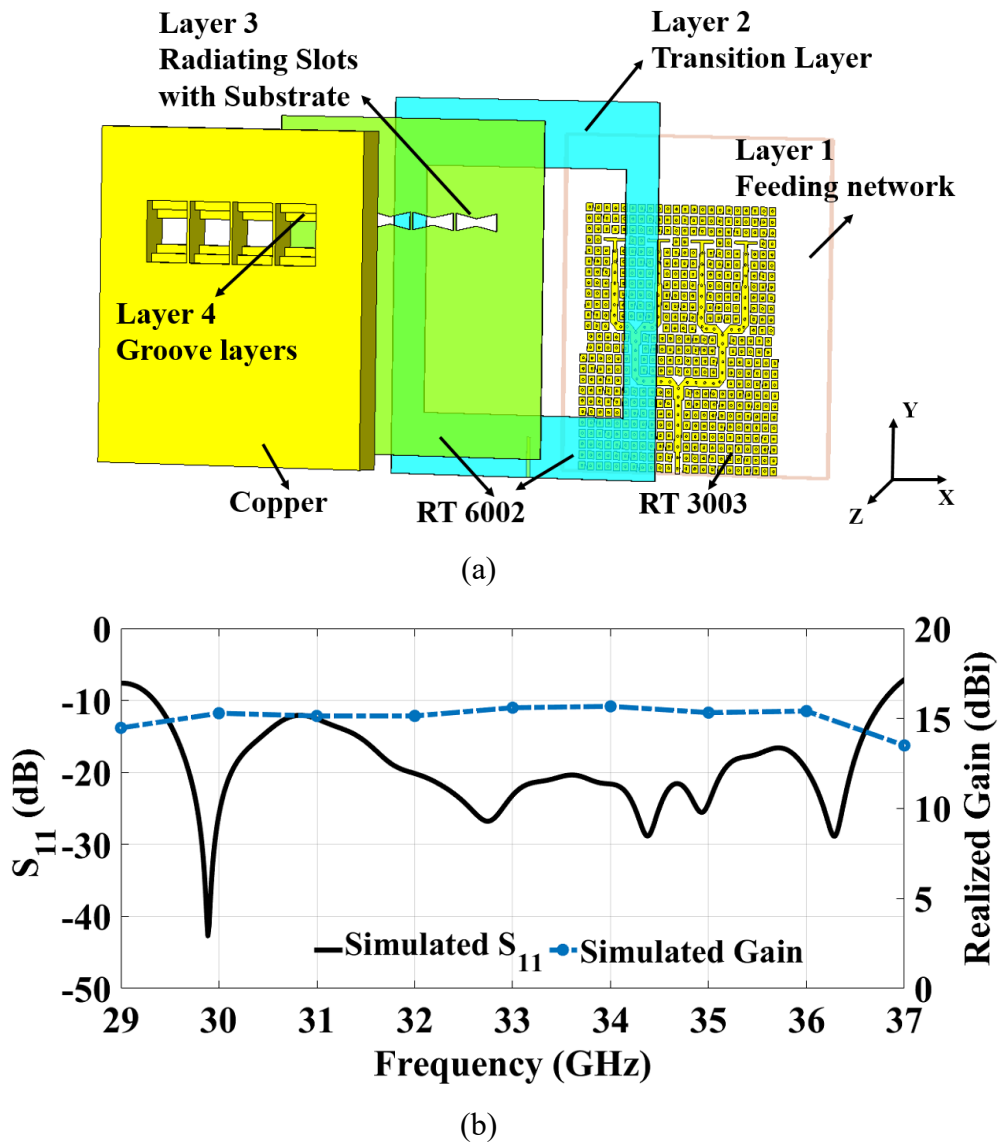


Figure 4.5: (a) Proposed, 1×4 three layer groove array antenna, (b) Simulated reflection coefficient and gain of 1×4 groove antenna array.

The proposed 1 x 4 linear groove antenna array is covering a wide bandwidth of 22% from (29.4-36.8) GHz. Also, the proposed array achieves a gain of 14.5 ± 1 dBi over the whole frequency band. Here it should be mentioned that the transition layer has a dual purpose, firstly to feed the waveguide and secondly to maintains the required air gap for PRGW. The radiation patterns of the linear groove antenna array for E- & H-plane are illustrated for various frequencies in Fig. 4.6 (a) and Fig. 4.6 (b) respectively.

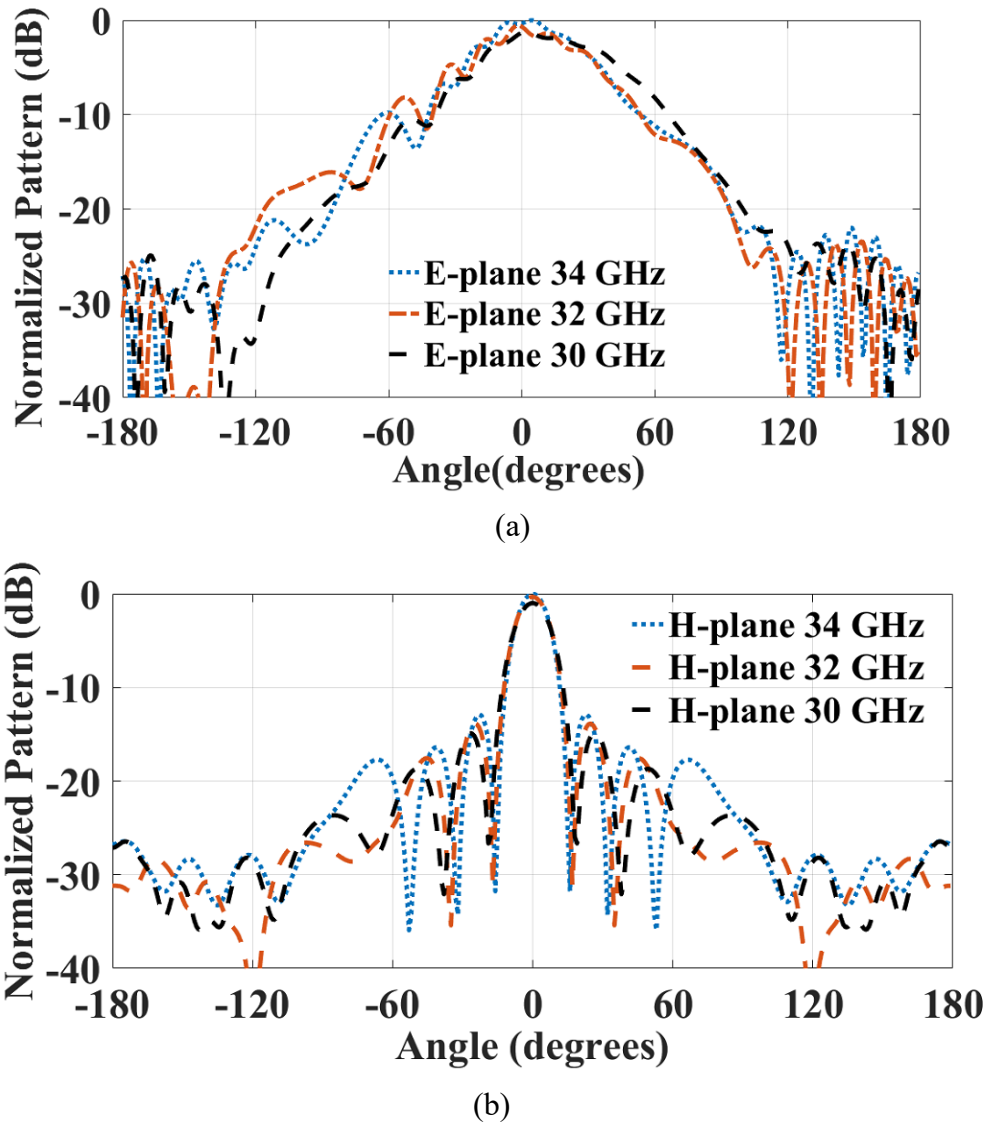


Figure 4.6: Simulated normalized radiation pattern for 1 x 4 linear array (a) E-plane, (b) H-plane.

In our proposed design, the orientation of the antenna elements is in the x-direction, where XZ-plane and YZ-plane are the H- and E-planes, respectively. These results in narrower beam width in the H-plane, while a wide beam width is achieved in the E-plane. As a result, the radiation pattern is affected in the E-plane as the groove edges in the y-direction are close to the antenna element, which results in a slight stable radiation pattern in the E-plane. Without increasing the overall antenna dimension, we have added a corrugation layer with a depth of $\lambda_0 / 4$ to improve the E-plane radiation pattern. This corrugation layer acts as an artificial magnetic ring surrounding the antenna array, which decreases the diffractions and accordingly enhances the radiation pattern. The improved linear array structure illustrated in Fig 4.7 with a corrugation layer and the improvement in the E-plane patterns are shown in Fig 4.8(a) & 4.8(b), at 32 and 34 GHz respectively.

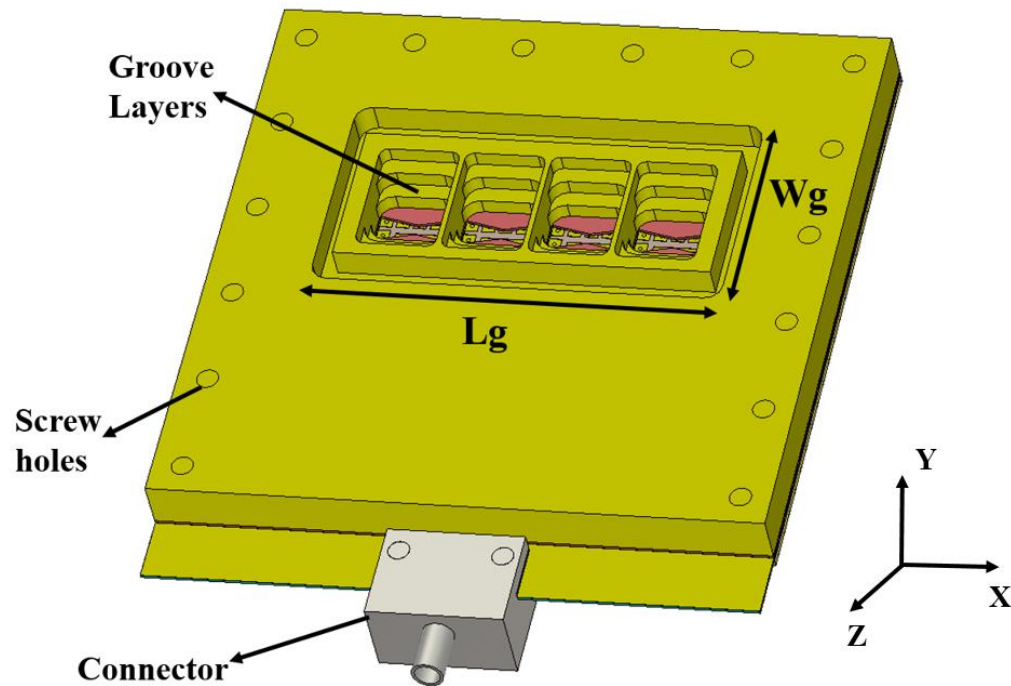
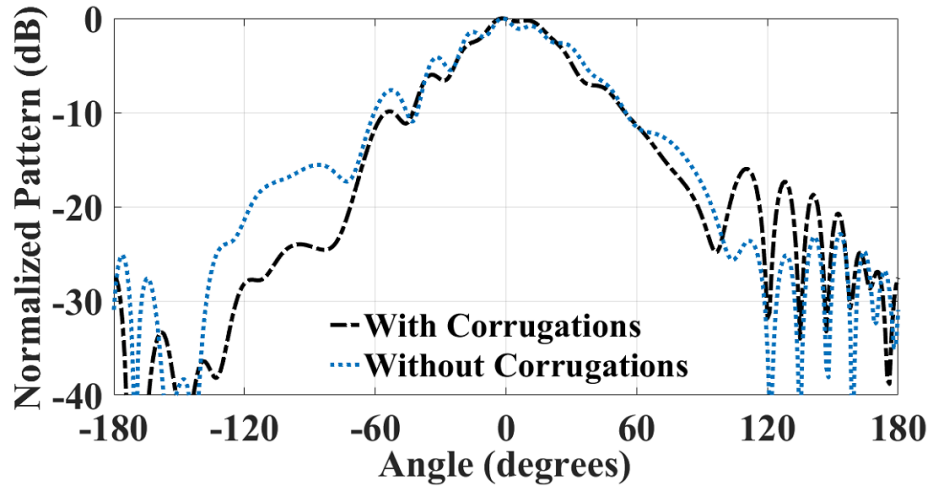
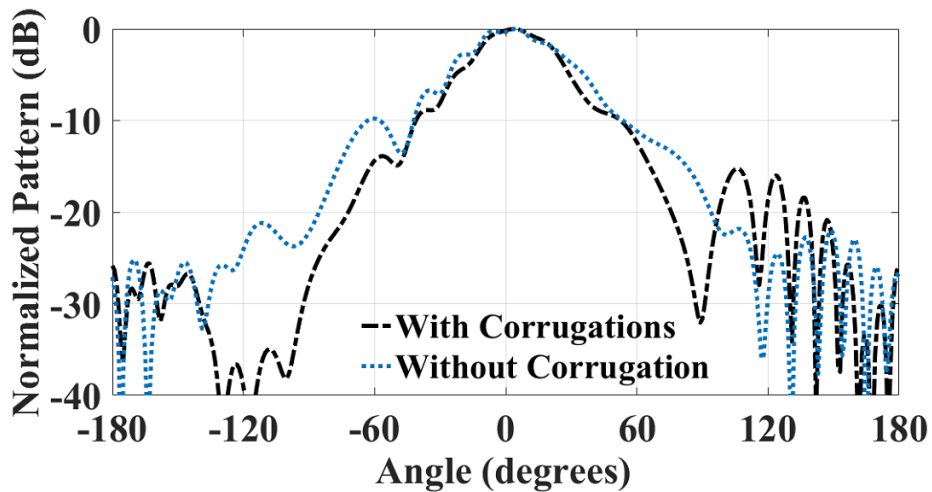


Figure 4.7: Improved 3-D, 1 x 4 groove antenna array with a corrugation ring.



(a)



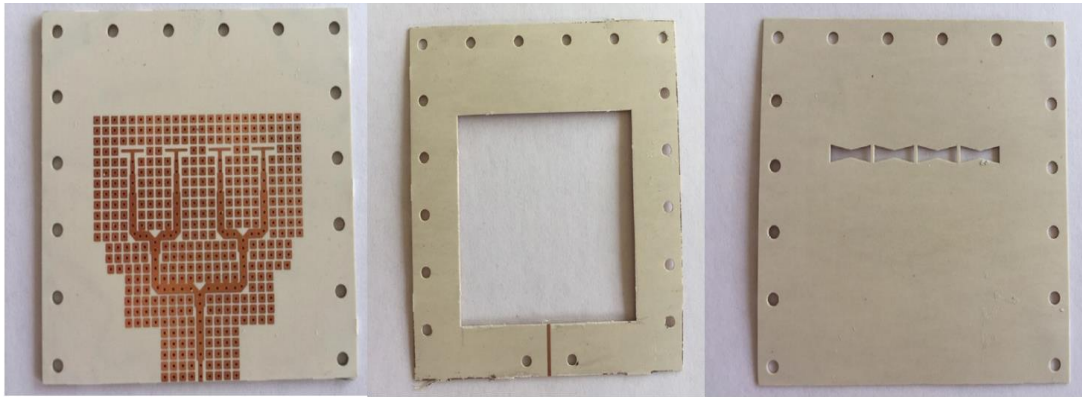
(b)

Figure 4.8: Simulated normalized radiation pattern at E-plane using a corrugation ring. (a) 32 GHz. (b) 34 GHz.

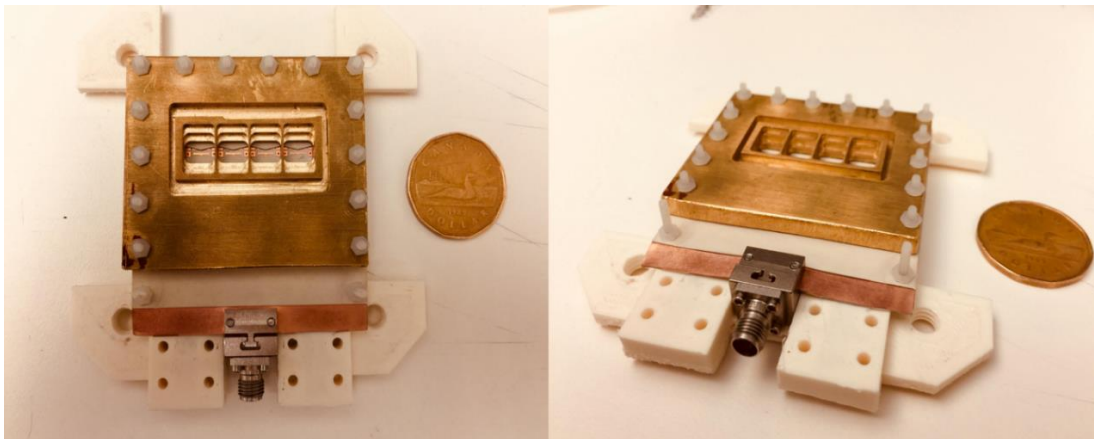
By adding the single corrugation layer, the E-plane radiation pattern improved significantly without increasing the antenna dimensions. This corrugation technique is generally applied to reduce side-lobe levels and to reduce cross polarizations. Adding a few more groove layers could have cut the edge diffractions more and improve the radiation pattern more. However, the design complexity will be more; that is why we have just focused on one layer.

4.5 Experimental and Validation

To validate the proposed design an array of 1 x 4 linear antenna is fabricated and measured where the photos of the fabricated parts are illustrated in Fig. 4.9 (a). Fabricated layers are assembled using plastic screws, where the assembling of the prototype is shown in Fig. 4.9 (b).



(a)

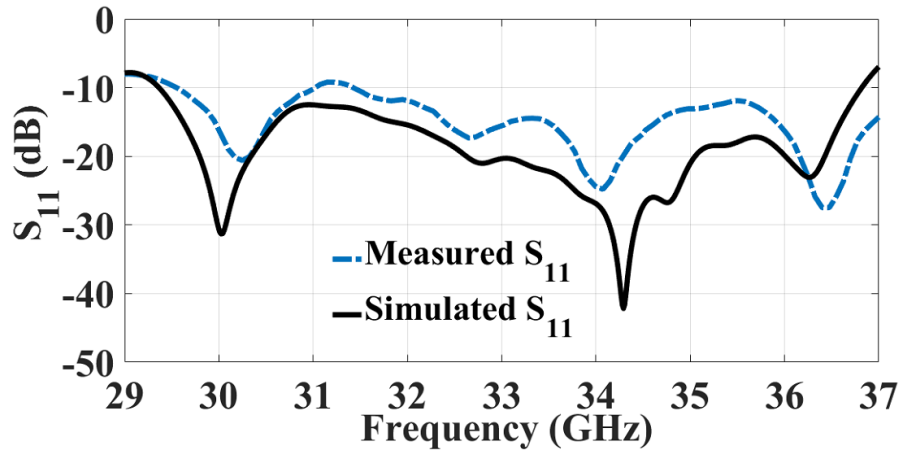


(b)

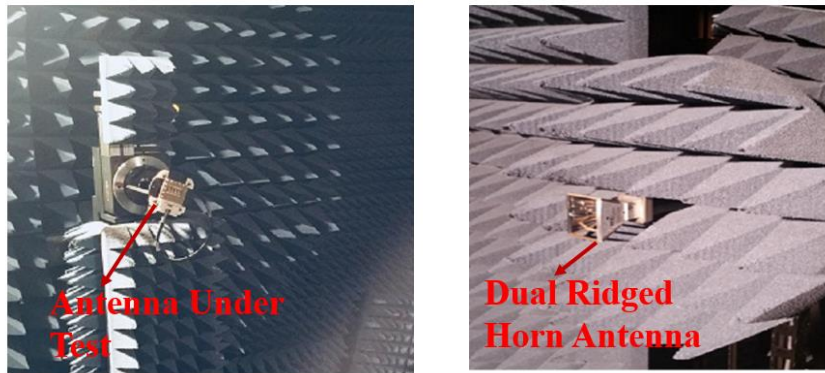
Figure 4.9: (a) Prototype layers. (b) Final assembly of 1 x 4 integrated antenna array.

The reflection coefficient is measured using an N52271A phase network analyzer, where the measured and simulated reflection coefficient are illustrated in Fig. 4.10 (a). A 22 % impedance bandwidth with $S_{11} < -10$ dB are achieved using the proposed prototype, where

there is a slight shift in the frequency response occurred with a small mismatch in (31-31.5) GHz. The gain and radiation pattern are measured in the anechoic chamber system, as shown in Fig. 4.10(b).



(a)



(b)

Figure 4.10: (a) Measured reflection coefficient of the fabricated 1 x 4 antenna array. (b) Radiation pattern measurement setup in the anechoic chamber.

It is worth mentioning that, in our measurement setup we don't have the facility to calculate measured radiation efficiency. The measured and simulated gain of the proposed array is shown in Fig. 4.11. This figure shows that the measured gain is 15 ± 1 dBi, where, fabrication tolerance for antenna layers as well as the groove may affect the measured

results. The measured radiation patterns in the E- and H-plane are illustrated in Fig. 4.12 and 4.13 respectively at 30 and 34 GHz.

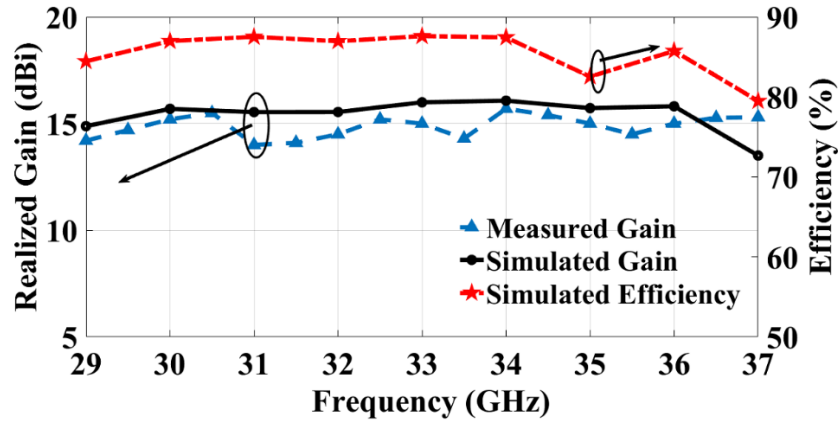
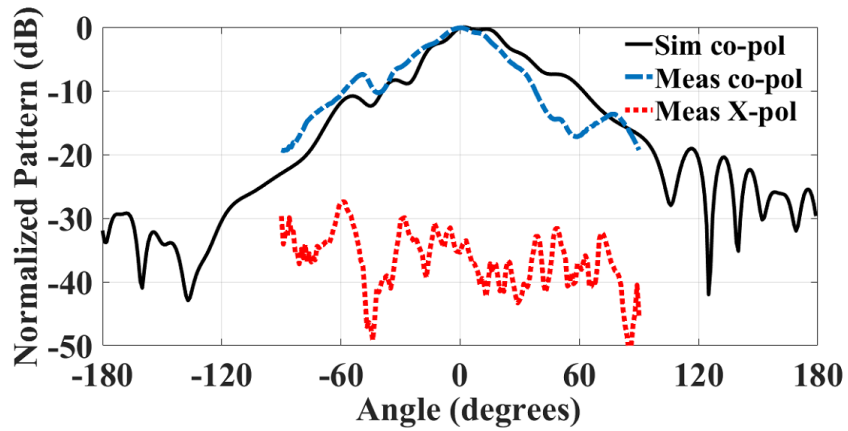
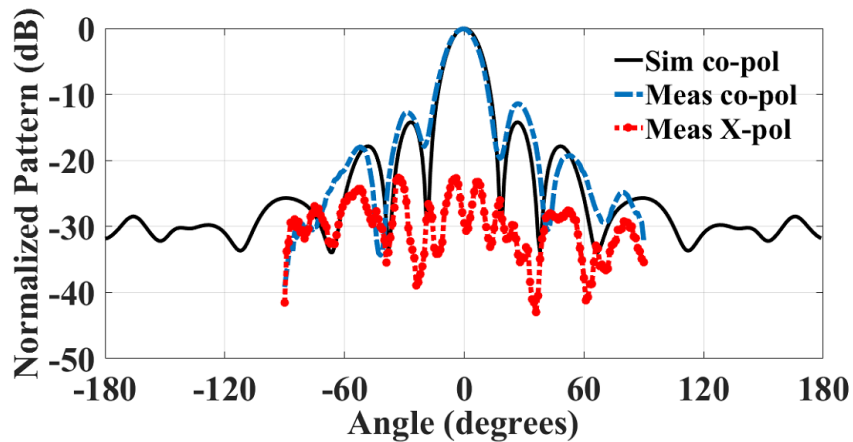


Figure 4.11: Measured gain of the fabricated 1 x 4 antenna array.

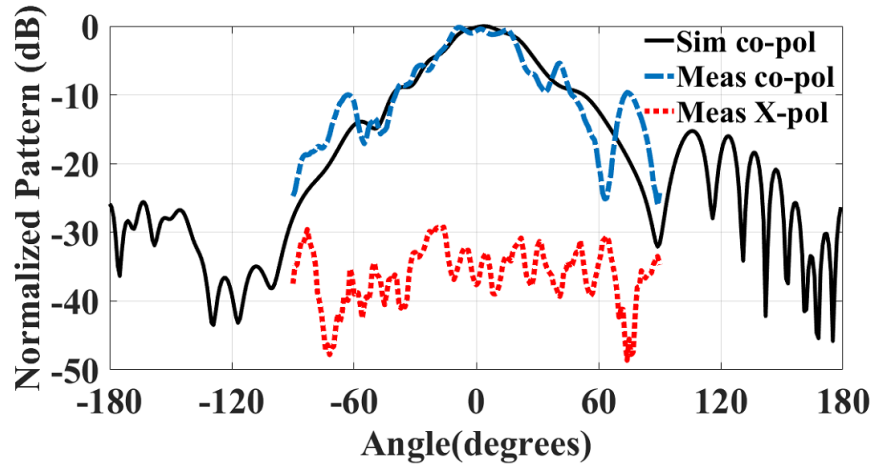


(a)

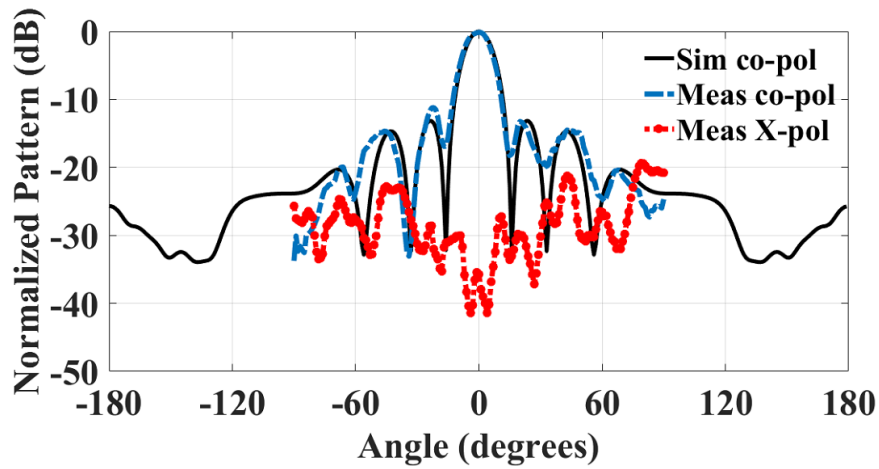


(b)

Figure 4.12: Comparison of measured and simulated E- and H-plane pattern at 30 GHz.



(a)



(b)

Figure 4.13: Comparison of measured and simulated E and H-plane pattern at 34 GHz.

The measured co-polarizations of the antenna in both the E- and H-plane are in a good agreement, and the cross polarization levels are low in both the E- and H-plane. The fabricated prototype achieves a gain of 15.5 dBi and a radiation efficiency higher than 80% over the operating frequency bandwidth where table 4.2 shows a comparison between the proposed work and previous works. The proposed antenna exhibits superior characteristics at mm-wave frequency bands including low loss, self-packaged and planar structure. In [46], the SIW cavity antenna array suffers from the grating lobes where the SLL is less

than -6.5 dB at high frequencies, which restricts its application. In addition, for 2D beam scanning purpose, ME dipole array was fed by RGW Butler matrix to provide stable radiation pattern and higher bandwidth [45]. However, the gain and radiation efficiency of the antenna is low compared to our work. An array of 1 x 8 aperture coupled ME dipole was proposed in [70], for circular polarization applications, however, the ME dipole antenna provides only 14.5 % bandwidth and the size of the antenna is enormous compared to our proposed antenna. In [43], 4 x 4 ME dipole antenna was used for high gain and wideband purpose, however, the bandwidth is less than our proposed work. Our proposed antenna provides wideband, high gain, better efficiency as well as strong mechanical support compared to the other published designs.

Table 4.2: Comparison of proposed antenna with some previously published work

Ref	Frequency (GHz)	Antenna Type	Size (λ_0)	BW (%)	Gain (dBi)	Rad. efficiency
This work	30	1 x 4 Slot Antenna	$4\lambda_0 \times 4.2 \lambda_0 \times 0.53 \lambda_0$	22	15.5	87% simulated
[59]	60	SIW Cavity	Not mentioned	16	21	Not mentioned
[58]	30	2 x 2 ME dipole	$5.6 \lambda_0 \times 7.1 \lambda_0 \times 0.28 \lambda_0$	20	10.3	84% simulated
[77]	95	1 x 8 ME dipole	$8.25 \lambda_0 \times 5.4 \lambda_0 \times 3.6 \lambda_0$	14.5	16.5	Not mentioned
[56]	30	4 x 4 ME dipole	$3.5 \lambda_0 \times 3.4 \lambda_0 \times 0.28 \lambda_0$	16.5	21.2	70% measured

Chapter 5

Conclusion and Future Works

5.1 Conclusion

Ridge gap waveguide has already gained its prominence as a guiding structure in the millimeter and sub-millimeter wave applications. In this work, we have worked with the printed version of gap waveguide. Although, the performance of the metal ridge gap is better in terms of matching level as a vertical degree of freedom exists in all matching transformers. However, the CNC milling is expensive, which increase the overall cost of the system based on this technology. Hence, we have selected a more economical solution as a base technology for our work. PRGW is a packaged structure, so for the antenna to radiate it requires a radiation slot. Ideally, a slot antenna has a narrow bandwidth; in most cases, it is around 3-5 % bandwidth at the center frequency. To improve the bandwidth and gain simultaneously, we have proposed a two-section transformer, with a T-shaped ridge with a bow-tie slot antenna. The gain is enhanced using a rectangular shaped three-layered groove loaded just on top of the bow-tie slot.

In this work, we have presented a high gain, a wideband antenna array with a radiation efficiency of 87%, based on the PRGW technology. However, other designs reported based on this technology achieved efficiency much lower than our work. It has lower losses compared to printed microstrip lines. A bow-tie slot antenna is utilized to get a wide impedance bandwidth, while a three-layer groove structure is deployed to provide

substantial mechanical support and enhance the gain. The fabricated prototype achieves a high gain of 15.5 dB over the operating frequency bandwidth. On the other hand, other published design with ME dipole antenna array technology can provide a gain increase of 21 dBi with 4 x 4 elements. Moreover, similar technology arrays were reported to achieve 10.3 dBi gain. The fabricated prototype obtains 22% impedance bandwidth where both the measured and the simulated response are in a good agreement.

5.2 Future Works

This work can extend with integrating with beam forming network devices like couplers, phase shifters crossovers and antenna arrays which will be able to generate beams in different locations without any interference giving the same directivity. The phase shifters control the positioning of the beam, so interference between the propagating signals won't be an issue. In chapter 4, we have proposed a bow-tie shaped ridge which can be utilized for wideband applications. With the rising demand to use the 60 GHz band for high transfer rate communication, the PRGW can be a desirable candidate to realize the passive devices at this band or moreover, to be used as the standard guiding medium to integrate the complete systems. As gap waveguide is a packaged device, it could be possible to implement this technology in integrated circuits like MMIC, which can provide a better solution in terms of losses, and can reduce the mutual coupling between the circuit elements.

Reference

- [1] E. Dahlman, S. Parkvall, and J. Sköld, 4G LTE/LTE-Advanced for Mobile Broadband. Academic Press, 2011.
- [2] P. Zhouyue and F. Khan, "An introduction to millimeter-wave mobile broadband Systems," *IEEE Communications Magazine*, vol. 49, no. 6, pp. 101–107, June 2011.
- [3] M. G. Kachhavay and Ajay P. Thakare, "5G Technology- Evolution and Revolution" *International Journal of Computer Science and Mobile Computing*, vol. 3, no. 3, pp. 1080-1087, Mar. 2014.
- [4] T. S. Rappaport *et al.*, "Millimeter Wave Mobile Communications for 5G Cellular: It Will Work," in *IEEE Access*, vol. 1, pp. 335-349, May 2013.
- [5] M. Elsaadany, A. Ali and W. Hamouda, "Cellular LTE-A Technologies for the Future Internet-of-Things: Physical Layer Features and Challenges," in *IEEE Communications Surveys & Tutorials*, vol. 19, no. 4, pp. 2544-2572, Fourthquarter 2017.
- [6] Y. Wang, J. Li, L. Huang, Y. Jing, A. Georgakopoulos, and P. Demestichas, "5G mobile: Spectrum broadening to higher-frequency bands to support high data rates," *IEEE Veh. Technol. Mag.*, vol. 9, no. 3, pp. 39-46, Sep. 2014.
- [7] Huang, K.-C., and D.J. Edwards, Millimeter Wave Antennas for Gigabit Wireless Communications, New York: John Wiley & Sons, 2008.
- [8] M. Marcus and B. Pattan, 'Millimeter Wave Propagation; Spectrum Management Implications', *IEEE Microwave Magazine*, no. 6, pp. 54-62, June 2005.
- [9] G. R. MacCartney, J. Zhang, S. Nie and T. S. Rappaport, "Path loss models for 5G millimeter wave propagation channels in urban microcells," *IEEE Global Communications Conference*, Atlanta, GA, pp. 3948-3953, Dec. 2013.
- [10] David M. Pozar, Microwave Engineering, 4th Edition, Wiley, 2011.
- [11] Y. Li, H. Wei, H. Guang, J. Chen, W. Ke, and T.-J. Cui, "Simulation and experiment Experiment on SIW slot array antennas," *IEEE Microw. Wireless Components Lett.*, vol. 14, no. 9, pp. 446–448, Aug. 2004.
- [12] J. Hirokawa and M. Ando, "Single-layer feed waveguide consisting of posts for Plane TEM wave excitation in parallel plates," *IEEE Transactions on Antennas*

- and Propagation*, vol. 46, no. 5, pp. 625–630, May 1998.
- [13] P. S. Kildal, E. Alfonso, A. Valero-Nogueira and E. Rajo-Iglesias, "Local Metamaterial Based Waveguides in Gaps between Parallel Metal Plates," in *IEEE Antennas and Wireless Propagation Letters*, vol. 8, pp. 84-87, Jan. 2009.
- [14] O. H. Hassan, S. I. Shams and A. M. M. Allam, "Dual Band Circularly polarized Antenna with CPW Feeding structure". In *Asia Pacific Microwave Conference – (APMC)*, pp. 2052 - 2055, Dec. 2010.
- [15] R.A. El-adl, M. H. Sharaf, S. I. Shams, A. M. M. Allam, "An arrow shaped printed antenna for ZigBee applications" in *Antennas and Propagation Society International Symposium (APS/URSI)*, Chicago, pp. 1-2, July 2012.
- [16] S. D. Targonski, R. B. Waterhouse and D. M. Pozar, "Design of wide-band aperture stacked patch microstrip antennas," in *IEEE Trans. Antennas Propag.*, vol. 46, No. 9, pp. 1245-1251, Sep. 1998.
- [17] R. B. Waterhouse, D. Novak, A. Nirmalathas, and C. Lim, "Broadband printed Mm-wave antennas," in *IEEE Trans. Antennas Propag*, vol. 51, no. 9, pp. 2492- 2495, Sep. 2003.
- [18] M. A. Fattah, S. I. Shams and A. M. M. Allam, "Irregular Pentagon Monopole Structured Antenna for Ultra-wideband Communication Systems", *1st Middle East Conference on Antennas and Propagation (MECAP)*, Cairo, Oct. 2010.
- [19] M. A. Issa, M. H. Sharaf, S. I. Shams and A. M. M. Allam, "Stair-monopole antenna and irregular pentagon antenna in ultra-wideband applications" *IEEE International symposium Antenna Propagation Society*, pp. 1766-1769, July 2011.
- [20] M. M. Azer, S. I. Shams, and A. M. M. Allam,. "Compact Double-Sided Printed Omni Directional Ultra-Wideband Antenna" in *14th International Symposium on Antenna Technology and Applied Electromagnetic (ANTEM)*, Ottawa, July 2010.
- [21] Q. X. Chu, X. R. Li and M. Ye, "High-Gain Printed Log-Periodic Dipole Array Antenna with Parasitic Cell for 5G Communication," in *IEEE Transactions on Antennas and Propagation*, vol. 65, no. 12, pp. 6338-6344, Dec. 2017.
- [22] S. M. Sifat, S. I. Shams and A. R. Sebak, "High Gain Wideband Log Periodic Dipole Array Antenna Loaded with Corrugations," *18th International Symposium on Antenna Technology and Applied Electromagnetics (ANTEM)*, Waterloo, ON,

- Canada, pp. 1-2. Aug. 2018.
- [23] Constantine A. Balanis, “Antenna Theory: Analysis and Design”, 3rd Edition, NJ, USA: Wiley, 2005.
- [24] Warren L. Stutzman, Gary A. Thiele, “Antenna Theory and Design”, 3rd Edition, USA, Wiley, May 2012.
- [25] L. Lucci, R. Nesti, G. Pelosi, and S. Selleri, “A Stackable constant-width corrugated horn design for High-Performance and Low-Cost Feed Arrays at Mm-wavelengths” *IEEE Antennas and Wireless Propag. Lett.*, vol. 11, pp. 1162-1165, Sep. 2012
- [26] N. Ghassemi and K. Wu, “Millimeter-Wave Integrated Pyramidal Horn Antenna Made of Multilayer Printed Circuit Board (PCB) Process,” in *IEEE Transactions on Antennas and Propagation*, vol. 60, no. 9, pp. 4432–4435, July 2012.
- [27] G. M. Rebeiz, D. P. Kasilingam, Y. Guo, P. A. Stimson and D. B. Rutledge, "Monolithic Millimeter-wave two-dimensional horn imaging arrays," *IEEE Transactions on Antennas and Propagation*, vol. 38, no. 9, pp. 1473-1482, Sep. 1990.
- [28] Ke Wu, D. Deslandes and Y. Cassivi, "The substrate integrated circuits - a new concept for high-frequency electronics and optoelectronics," *6th International Conference on Telecommunications in Modern Satellite, Cable and Broadcasting Service, 2003. TELSIKS*, pp. P-III-P-X vol.1, Oct. 2003.
- [29] D.Y. Kim, W. Chung, C. Park, S. Lee, and S. Nam, “Design of a 45- Inclined SIW Resonant Series Slot Array Antenna for-Band,” in *IEEE Antennas Wireless Propag. Lett.* vol. 10, pp. 318-321, April 2011.
- [30] E.Y. Jung, J.W. Lee, T.K. Lee, and W.K. Lee, “SIW-based array antennas with sequential feeding for X-band satellite communication,” in *IEEE Trans. Antennas Propag.*, vol. 60, no. 8, pp. 3632-3639, May 2012.
- [31] G.Q. Luo, Z.F. Hu, Y. Liang, L.Y. Yu, and L.L. Sun, “Development of low profile cavity backed crossed slot antennas for planar integration,” *IEEE Trans. Antennas Propag.*, vol. 57, no. 10, 2972-2979, Sep. 2009.
- [32] P. S. Kildal, “Artificially soft and hard surfaces in electromagnetics,” *IEEE Transactions on Antennas and Propagation*, vol. 38, no. 10, pp. 1537–1544, Oct. 1990.
- [33] D. J. Salomonsson, J. Hirokawa, P. S. Kildal, and A. Tengs, “Corrugated soft sector horn with different beam properties in the two principal planes,” *IEEE Proceedings*

- Microwaves, Antennas and Propagation*, vol. 144, no. 1, pp. 13–19, Feb. 1997.
- [34] E. Lier and P. S. Kildal, “Soft and hard horn antennas,” *IEEE Transactions on Antennas and Propagation*, vol. 36, no. 8, pp. 1152–1157, Aug. 1988.
- [35] M. G. Silveirinha, C. A. Fernandes, and J. R. Costa, “Electromagnetic charecteriza-tion of textured surfaces formed by metallic pins,” *IEEE Trans. Antennas Propag.*, vol. 56, no. 2, pp. 405–415, Feb. 2008.
- [36] S. I. Shams and A. A. Kishk, "Determining the Stopband of a Periodic Bed of nails from the Dispersion Relation Measurements Prediction," *IEEE Trans. Compon., Packaging, Manufacturing Techn.*, vol. 7, no. 4, pp. 621-629, April. 2017.
- [37] P. S. Kildal, "Three metamaterial-based gap waveguides between parallel metal plates for mm/submm waves," *3rd European Conference on Antennas and Propagation.*, pp. 28-32, Berlin, Mar. 2009.
- [38] P. S. Kildal, A. U. Zaman, E. Rajo-Iglesias, E. Alfonso and A. Valero-Nogueira "Design and experimental verification of ridge gap waveguide in bed of nails for Parallel-plate mode suppression," in *IET Microwaves, Antennas and Propagation* vol. 5, no. 3, pp. 262-270, Feb. 2011.
- [39] A. A. Brazález, E. Rajo-Iglesias, J. L. Vázquez-Roy, A. Vosoogh, and P.-S. Kildal "Design and validation of microstrip gap waveguides and their transitions to rectangular waveguide, for millimeter-wave applications," *IEEE Trans. Microw. Theory Techn.*, vol. 63, no. 12, pp. 4035-4050, Dec. 2015.
- [40] S. I. Shams, A. A. Kishk, “Printed texture with triangle flat pins for bandwidth enhancement of the ridge gap waveguide” *IEEE Trans. Microw. Theory Techn.*, vol.7, pp. 2093-2100, Jan. 2017.
- [41] M. Bosiljevac, A. Polemi, S. Maci, and Z. Sipus, “Analytic approach to the analysis of ridge and groove gap waveguides - comparison of two methods,” in Proc. of the 5th European Conference on Antennas and Propagation, EuCAP, pp. 1886–1889, Mar. 2011.
- [42] A. U. Zaman, A. Kishk, and P. S. Kildal, “Narrow-band microwave filter using high Q groove gap waveguide resonators without sidewalls,” *IEEE Transactions on Components, Packaging and Manufacturing Technology*, vol. 2, no. 11, pp. 1882–1888, 2011.

- [43] E. Pucci, E. Rajo-Iglesias, J. Vázquez-Roy and P. Kildal, "Planar Dual-Mode Horn Array With Corporate-Feed Network in Inverted Microstrip Gap waveguide" in *IEEE Transactions on Antennas and Propagation*, vol. 62, no. 7, pp. 3534-3542, July, 2014.
- [44] A. U. Zaman and P. S. Kildal, "Wide-Band Slot Antenna Arrays With Single Layer Corporate-Feed Network in Ridge Gap Waveguide Technology," in *IEEE Trans. Antennas Propag.* vol. 62, no. 6, pp. 2992-3001, June 2014.
- [45] M. A. Sharkawy and A. A. Kishk, "Long Slots Array Antenna Based on Ridge Gap Waveguide Technology," *IEEE Trans. Antennas Propag.*, vol. 62, no. 10, pp. 5399-5403, Oct. 2014
- [46] M. Al Sharkawy and A. A. Kishk, "Wideband Beam-Scanning Circularly Polarized Inclined Slots Using Ridge Gap Waveguide," in *IEEE Antennas and Wireless Propagation Letters*, vol. 13, pp. 1187-1190, June 2014.
- [47] S. I. Shams, M. A. Abdelaal and A. A. Kishk, "Broadside uniform leaky-wave slot array fed by ridge gap splitted line," *IEEE International Symposium on Antennas and Propagation & USNC/URSI National Radio Science Meeting*, Vancouver, pp. 2467-2468, July 2015.
- [48] D. Zarifi, A. Farahbakhsh, A. U. Zaman and P. S. Kildal, "Design and Fabrication of a High Gain 60 GHz Corrugated Slot Antenna Array with Ridge Gap Waveguide Distribution Layer," *IEEE Trans. Antennas Propag.*, vol. 64, no.7, pp. 2905-2913, July 2016.
- [49] M. S. Sorkherizi and A. A. Kishk, "Lowloss planar bandpass filters for millimeter-wave application", in *IEEE MTT-S Int. Microw. Symp. Dig.*, pp. 1-4, May 2015.
- [50] M. S. Sorkherizi, A. Khaleghi and P. S. Kildal, "Direct-Coupled Cavity Filter in Ridge Gap Waveguide," in *IEEE Transactions on Components, Packaging and Manufacturing Technology*, vol. 4, no. 3, pp. 490-495, Mar. 2014.
- [51] S. I. Shams and A. A. Kishk, "Design of 3-dB Hybrid Coupler Based on RGW Technology," *IEEE Trans. Microw. Theory Techn.*, vol. 65, no.10, pp. 3849-3855, Oct. 2017.
- [52] M. M. M. Ali, S. I. Shams and A. R. Sebak, "Printed Ridge Gap Waveguide 3-dB Coupler: Analysis and Design Procedure," in *IEEE Access*, vol. 6, pp. 8501-8509,

July 2018.

- [53] M. M. M. Ali, S. I. Shams, A. Sebak and A. A. Kishk, "Rectangular Waveguide Cross-Guide Couplers: Accurate Model for Full-Band Operation," *IEEE Microwave and Wireless Components Letters*, vol. 28, no. 7, pp. 561-563, July 2018.
- [54] S. I. Shams and A. A. Kishk, "Wide band power divider based on Ridge gap Waveguide "17th International Symposium on Antenna Technology and Applied Electromagnetics (ANTEM), Montreal, QC, pp. 1-2, July 2016.
- [55] N. Ashraf, A. A. Kishk and A. Sebak, "Broadband Millimeter-Wave Beamforming Components Augmented With AMC Packaging," in *IEEE Microwave and Wireless Components Letters*, vol. 28, no. 10, pp. 879-881, Oct. 2018.
- [56] M. Sharifi. Sorkherizi, A. Dadgarpour and A. A. Kishk, "Planar High-efficiency Antenna Array Using New Printed Ridge Gap Waveguide Technology," in *IEEE Trans. Antennas Propag.*, vol. 65, no. 7, pp. 3772-3776, July 2017.
- [57] H. Attia, M. S. Sorkherizi and A. A. Kishk, "60 GHz slot antenna array based on ridge gap waveguide technology enhanced with dielectric superstrate," *9th European Conference on Antennas and Propagation (EuCAP)*, Lisbon, pp. 1-4, Mar. 2015.
- [58] M. M. M. Ali and A. Sebak, "2-D Scanning Magneto electric Dipole Antenna Array Fed by RGW Butler Matrix," *IEEE Trans Antennas Propag.*, vol. 66, no. 11, pp. 6313-6321, Nov. 2018.
- [59] S. A. Razavi, P. S. Kildal, L. Xiang, E. Alfonso Alós and H. Chen, "2 x 2-Slot Element for 60-GHz Planar Array Antenna Realized on Two Doubled-Sided PCBs Using SIW Cavity and EBG-Type Soft Surface fed by Microstrip-Ridge Gap Waveguide," *IEEE Transactions on Antennas and Propagation*, vol. 62, no. 9, pp. 4564- 4573, Sep. 2014.
- [60] M. M. M. Ali and A. R. Sebak, "4× 2-slot element for 30-GHz planar array Antenna realized using SIW cavity and fed by microstrip line line-ridge gap waveguide" in *IEEE International Symposium on Antennas and Propagation & USNC/URSI National Radio Science Meeting*, San Diego, CA, pp. 2149-2150, July 2017.
- [61] S. I. Shams, M. A. Abdelaal and A. A. Kishk, "SIW magic tee fed by printed Ridge Gap Waveguide Design," *17th International Symposium on Antenna Technology and Applied Electromagnetics (ANTEM)*, Montreal, pp. 1-2, July 2016.
- [62] Y. Al-Alem and A. A. Kishk, "Highly Efficient Unpackaged 60 GHz Planar Antenna

- Array," in *IEEE Access*, vol. 7, pp. 19033-19040, Jan. 2019.
- [63] N. Bayat-Makou and A. A. Kishk, "Millimeter-Wave Substrate Integrated Dual Level Gap Waveguide Horn Antenna," in *IEEE Transactions on Antennas and Propagation*, vol. 65, no. 12, pp. 6847-6855, Dec. 2017.
- [64] H. Raza, J. Yang, P.-S. Kildal, and E. A. Alos, "Microstrip-ridge gap waveguide study of losses, bends, and transition to WR-15," *IEEE Trans. Microw. Theory Techn.*, vol. 62, no. 9, pp. 1943-1952, Sep. 2014.
- [65] E. Pucci, E. Rajo-Iglesias and P. S. Kildal, "New Microstrip Gap Waveguide on Mushroom-Type EBG for Packaging of Microwave Components," *IEEE Microw. and Wireless Compon. Lett.*, vol. 22, no. 3, pp. 129-131, Mar. 2012.
- [66] M. S. Sorkherizi and A. A. Kishk, "Fully printed gap waveguide with facilitated design properties," *IEEE Microw. Wireless Compon. Lett.*, vol. 26, no. 9, pp. 657-659, Sep. 2016.
- [67] M. Sharifi Sorkherizi and A. A. Kishk, "Transition from microstrip to printed ridge gap waveguide for millimeter-wave application," *IEEE International Symposium on Antennas and Propagation & USNC/URSI National Radio Science Meeting*, Vancouver, BC, pp. 1588-1589, July 2015.
- [68] S. I. Shams and A. A. Kishk, "Wideband Coaxial to Ridge Gap Waveguide transition," in *IEEE Trans. Microw. Theory Techn.*, vol. 64, no. 12, pp. 4117-4125, Dec. 2016.
- [69] S. I. Shams and A. A. Kishk, "Ridge gap waveguide to microstrip line transition with perforated substrate," *USNC-URSI Radio Science meeting (Joint with AP-S Symposium)*, Memphis, TN, pp. 215-215, July 2014.
- [70] I. Afifi, M. M. M. Ali and A. Sebak, "Analysis and Design of a Wideband Coaxial Transition to Metal and Printed Ridge Gap Waveguide," in *IEEE Access*, vol. 6, pp. 70698-70706, Dec. 2018.
- [71] M. M. M. Ali and A. Sebak, "Compact Printed Ridge Gap Waveguide Crossover for Future 5G Wireless Communication System," in *IEEE Microwave and Wireless Components Letters*, vol. 28, no. 7, pp. 549-551, July 2018.
- [72] S. I. Shams, M. M. Tahseen and A. A. Kishk, "Wideband Relative Permittivity Characterization of Thin Low Permittivity Textile Materials Based on Ridge Gap

- Waveguides," in *IEEE Transactions on Microwave Theory and Techniques*, vol. 64, no. 11, pp. 3839-3850, Nov. 2016.
- [73] M. M. M. Ali, S. I. Shams and A. Sebak, "Reconfigurable Antenna Based on Printed Ridge Gap Waveguide Technology," *18th International Symposium on Antenna Technology and Applied Electromagnetics (ANTEM)*, Waterloo, ON, pp. 1-2, Aug. 2018.
- [74] S. I. Shams, M. M. M. Ali and A. Sebak, "Reconfigurable Guiding Structure Based on Printed Ridge Gap Waveguide Technology," *18th International Symposium on Antenna Technology and Applied Electromagnetics (ANTEM)*, Waterloo, ON, pp. 1-2, July 2018.
- [75] S. M. Sifat, M. M. M. Ali, S. I. Shams and A. Sebak, "High Gain Bow-Tie Slot Antenna Array Loaded With Grooves Based on Printed Ridge Gap Waveguide Technology," in *IEEE Access*, vol. 7, pp. 36177-36185, Mar. 2019.
- [76] FEDERAL COMMUNICATIONS COMMISSION OFFICE OF ENGINEERING AND TECHNOLOGY POLICY AND RULES DIVISION, pp. 55-57, Oct, 2018.
- [77] J. Cao, H. Wang, S. Mou, S. Quan and Z. Ye, "W-Band High-Gain Circularly Polarized Aperture-Coupled Magneto-Electric Dipole Antenna Array with Gap Waveguide Feed Network," in *IEEE Antennas and Wireless Propagation Letters*, vol. 16, pp. 2155-2158, May 2017.